

**PURDUE UNIVERSITY
GRADUATE SCHOOL
Thesis/Dissertation Acceptance**

This is to certify that the thesis/dissertation prepared

By Alycia G. Berman

Entitled

Influence of Mechanical Stimulation on the Quantity and Quality of Bone During Modeling

For the degree of Master of Science in Biomedical Engineering

Is approved by the final examining committee:

Joseph M. Wallace

Chair

Sungsoo Na

Jiliang Li

To the best of my knowledge and as understood by the student in the Thesis/Dissertation Agreement, Publication Delay, and Certification Disclaimer (Graduate School Form 32), this thesis/dissertation adheres to the provisions of Purdue University's "Policy of Integrity in Research" and the use of copyright material.

Approved by Major Professor(s): Joseph M. Wallace

Approved by: Ken Yoshida

Head of the Departmental Graduate Program

7/6/2016

Date

INFLUENCE OF MECHANICAL STIMULATION ON THE QUANTITY AND
QUALITY OF BONE DURING MODELING

A Thesis

Submitted to the Faculty

of

Purdue University

by

Alycia G. Berman

In Partial Fulfillment of the

Requirements for the Degree

of

Master of Science in Biomedical Engineering

August 2016

Purdue University

Indianapolis, Indiana

ACKNOWLEDGMENTS

As is true of any effort, there is much work and a myriad of people who helped make this thesis possible. To begin, I would like to acknowledge my major professor, Dr. Joseph Wallace. He took me in as a sophomore even though I knew nothing about research and has been a constant support. He has put up with my (many) questions, has encouraged me to pursue my interests, and has challenged me to be better. I am very grateful for his support and encouragement throughout my time in his lab. I would also like to acknowledge my committee members, Dr. Sungsoo Na and Dr. Jiliang Li, for their time and support in this pursuit, as well.

Thanks, as well, to the members of the lab: Dr. Max Hammond, Silvia Canelón, Creasy Clauser, Jay Kadakia, Tyler Laine, Brian Frondorf, Ryan Geltz, and Jenny Cozad. Thank you for accepting me into the lab group, showing me the ropes, helping me smile even through the frustrations of trouble-shooting, providing advice as I tried to sort through data, and being there to celebrate accomplishments. In addition, specific to the projects mentioned in this thesis, I would like to acknowledge Dr. Max Hammond for his support in helping me understand statistics. Brian Frondorf helped with the in vivo portion of the low-dose BAPN tibial loading experiment (Chapter 2). Not only that, but after we found out that we were going to repeat the study at a higher dosage (Chapter 3), he was willing to stay and help me with that study, as well. I doubt that I would have been able to do the 14 weeks of daily injections had it not been for his assistance. Lastly, Jenny harvested the mice from the high-dose BAPN study (Chapter 3), which was a huge help.

Last, but certainly not least, I would like to thank my family. I could not ask for a better support system. You have seen me at my best and my worst, and have been there regardless. Thank you.

TABLE OF CONTENTS

	Page
LIST OF TABLES	vi
LIST OF FIGURES	vii
ABSTRACT	ix
1 INTRODUCTION	1
1.1 Abstract	1
1.2 Introduction	2
1.3 Historical Perspective and Clinical Significance	2
1.4 Animal Models of Mechanical Stimulation	4
1.4.1 Extrinsic Factors Influencing Bone Formation Response	5
1.4.2 Intrinsic Factors Influencing Bone Formation Response	6
1.4.3 Mechanical Stimulation in Pre-clinical Assessment	7
1.5 Quality Versus Quantity	8
1.6 Mechanical Stimulation and Bone Quality	9
1.7 Conclusion	12
1.8 Thesis Overview	12
1.9 References	14
2 IN VIVO TIBIAL LOADING OF OSTEOLATHRYTIC MICE INDUCED BY A LONG-TERM LOW-DOSE TREATMENT OF BAPN	23
2.1 Introduction	23
2.2 Methods	24
2.2.1 Animals	24
2.2.2 Strain Calibration	25
2.2.3 <i>In vivo</i> Loading	25
2.2.4 Micro Computed Tomography (μ CT)	26

	Page
2.2.5 Mechanical Testing	27
2.2.6 Fracture Toughness Testing	27
2.2.7 Statistics	28
2.3 Results	28
2.3.1 Animal Weight	28
2.3.2 Strain Calibration	29
2.3.3 Tibial Morphology	30
2.3.4 Tibial Mechanics	35
2.3.5 Fracture Toughness	36
2.4 Discussion	36
2.4.1 Little Effect of BAPN Treatment	36
2.4.2 Robust Bone Formation Response Due to Loading	40
2.4.3 Minimal Effects of Loading on Bone Quality	40
2.5 Conclusion	42
2.6 Acknowledgments	42
2.7 References	43
3 IN VIVO TIBIAL LOADING OF OSTEOLATHRYTIC MICE INDUCED BY A LONG-TERM HIGH-DOSE TREATMENT OF BAPN	45
3.1 Introduction	45
3.2 Methods	45
3.2.1 Animals	45
3.2.2 Strain Calibration	46
3.2.3 <i>In vivo</i> Loading	46
3.2.4 Micro Computed Tomography (μ CT)	46
3.2.5 Mechanical Testing	47
3.2.6 Statistics	47
3.3 Results	47
3.3.1 Animal Weight	47

	Page
3.3.2 Strain Calibration	48
3.3.3 Tibial Morphology	49
3.3.4 Tibial Mechanics	54
3.4 Discussion	57
3.4.1 Little Effect of BAPN Treatment	57
3.4.2 Robust Bone Formation Response Due to Loading	59
3.5 Conclusion	59
3.6 References	60
4 MODIFYING PARAMETERS AND SCHEDULE DURING AXIAL COMPRESSION OF THE MURINE TIBIA INCREASES BONE TISSUE QUALITY AND QUANTITY AND DECREASES ANIMAL DISCOMFORT	61
4.1 Introduction	61
4.2 Methods	63
4.2.1 Animals	63
4.2.2 <i>In vivo</i> Loading	63
4.2.3 Micro Computed Tomography (μ CT)	65
4.2.4 Fracture Toughness Testing	66
4.2.5 Statistics	66
4.3 Results	67
4.3.1 <i>In vivo</i> Assessment	67
4.3.2 CT Whole Limb Assessment	70
4.3.3 Cortical Analysis	71
4.3.4 Fracture Toughness Testing	73
4.4 Discussion	76
4.5 Conclusion	80
4.6 Acknowledgments	81
4.7 References	82
5 CONCLUSION AND FUTURE DIRECTIONS	84

LIST OF TABLES

Table	Page
2.1 Cortical morphology assessed by μ CT	33
2.2 Cancellous architecture assessed by μ CT	34
2.3 Structural-level bone mechanical properties	37
2.4 Tissue-level bone mechanical properties	38
2.5 Fracture stress intensity values assessed by fracture toughness	39
3.1 Cortical morphology assessed by μ CT	52
3.2 Cancellous architecture assessed by μ CT	53
3.3 Structural-level bone mechanical properties	55
3.4 Tissue-level bone mechanical properties	56
4.1 Summary of Groups	64
4.2 Limping Assessment Scale	65
4.3 Limping Assessment Week 1	67
4.4 Limping Assessment Week 2	68
4.5 Limping Assessment Week 3	68
4.6 Count of mice at each limping level after the final day of loading.	69
4.7 Joint stiffness at the end of the study.	69
4.8 Swollen ankle assessment at the end of the study.	70
4.9 Cortical morphology assessed by μ CT (MoTuWe High and MoTuWe Low groups)	74
4.10 Cortical morphology assessed by μ CT (MoWeFr and TuFr groups)	75

LIST OF FIGURES

Figure	Page
2.1 Strain calibration of BAPN and CON mice at 8 weeks of age indicate that CON mice had slightly stiffer bones (not significant). Loading the CON and BAPN mice to 11.1 N and 9.8 N, respectively, engendered $2100 \mu\epsilon$ in both groups.	29
2.2 During the 7-week study, significant growth occurred in (a) CON and (b) BAPN mice, especially in the first 4 weeks.	30
2.3 Cortical cross-section of the BAPN mice at (a) 8 weeks and (b) 11 weeks of age indicate that although there was slightly altered morphology in the BAPN mice at 8 weeks of age, those differences vanished at 11 weeks.	31
2.4 Cortical cross-sections in non-loaded and loaded limbs show a robust response of bone to load. Effects involve both periosteal expansion and cortical contraction.	32
2.5 Representative Force-Displacement and Stress-Strain curves show a robust response of load in terms of structure-level properties. When normalized by cross-sectional area, the effect of load is less pronounced. Treatment with BAPN had no effect on the mechanics.	35
3.1 Strain calibration of BAPN and CON mice at 8 weeks of age indicate similar stiffness in CON and BAPN mice. Loading the CON and BAPN mice to 9.6 N and 9.2 N, respectively, engendered $2100 \mu\epsilon$ in both groups.	48
3.2 During the 7-week study, significant growth occurred in (a) CON and (b) BAPN mice, especially in the first 4 weeks.	49
3.3 Cortical cross-section of the BAPN mice at (a) 8 weeks and (b) 11 weeks of age indicate slight, but consistent differences in the morphology of BAPN mice at 8 and 11 weeks of age.	50
3.4 Cortical cross-sections in non-loaded and loaded limbs show a robust response of bone to load. Effects involve both periosteal expansion and cortical contraction.	51
3.5 Representative Force-Displacement and Stress-Strain curves show a robust response of load in terms of structure-level properties. When normalized by cross-sectional area, the effect of load is less pronounced. Treatment with BAPN had no effect on the mechanics.	54

Figure	Page
4.1 Representative ex vivo μ CT scan of a mouse limb in the tibial loading fixture shows the orientation of the limb during loading.	64
4.2 The range of limping observed in the mice after the final day of loading clearly demonstrate that the MoTuWe High group had increased limping as compared to the other groups.	69
4.3 Scout scans of the MoTuWe High group show clear damage. The fibula is broken and the proximal metaphysis deformed in two of the mice. In addition, the epiphysis appears deformed in an additional two mice. Due to swollen ankles and limping after loading, the MoTuWe High group was not loaded on the last two days.	71
4.4 Scout scans of the MoTuWe Low group also show damage. The fibula is broken in one mouse and the proximal metaphysis deformed in two of the mice. In addition, the epiphysis appears deformed in an additional mouse. Two mice (indicated by the “*”) did not complete the loading regimen due to the assessment of pain.	72
4.5 Scout scans of the MoWeFr group lack the damage observed in the MoTuWe High and MoTuWe Low groups. All mice were able to be loaded the length of the study.	72
4.6 Scout scans of the TuFr group lack the damage observed in the MoTuWe High and MoTuWe Low groups. All mice were able to be loaded the length of the study.	73
4.7 Cortical cross-sectional areas in each of the groups shows an increase in bone mass in response to load.	76
4.8 Cortical thickness demonstrates the graded response due to loading in the four groups. MoTuWe High group had the greatest effect, followed by MoTuWe Low, MoWeFr, and lastly, TuFr. Interestingly, the MoTuWe High group also had increased variability. Significant differences ($p < 0.05$) are indicated by an “*”.	77
4.9 Graphs of fracture toughness parameters showing increasing crack stress intensity in the MoTuWe Low and MoWeFr groups at (a) yield force (crack initiation), (b) maximum force and (c) failure force (crack instability). Significant differences ($p < 0.05$) are indicated by an “*”.	78

ABSTRACT

Berman, Alycia G. M.S.B.M.E., Purdue University, August 2016. Influence of Mechanical Stimulation on the Quantity and Quality of Bone During Modeling. Major Professor: Joseph M. Wallace.

Skeletal fractures due to bone disease impact an estimated 1.5 million Americans per year, creating a large economic burden on our society. Treatment of bone diseases prior to fracture often involves bisphosphonates (current gold-standard in osteoporosis care and prevention). Although bisphosphonates decrease fracture incidence, they often improve bone mass without regard for bone quality. Thus, although bisphosphonates increase the amount of bone present, the inherent bone material strength often decreases, creating a trade-off that increases the risk of atypical fractures after long-term use. This trade-off demonstrates the need for a treatment that targets both bone quality AND quantity. Although bone quality is important, the components of bone that contribute to bone quality are incompletely understood, making it difficult to create new pharmacological agents. With this in mind, my particular area of interest is in understanding how mechanical stimuli protects the formation of bone, leading to improved bone quality. Initially, this area was explored through use of tibial loading in a disease mouse model (osteolathyrisms, induced by injection of β -aminopropionitrile) as a means of assessing how the body is able to compensate for decreased bone quality. The results of the BAPN and tibial loading studies indicated that injecting mice with BAPN may not be the ideal method to induce osteolathyrisms. However, other intriguing results from the BAPN studies then led us into an exploration of how tibial loading itself contributes to bone quality.

1. INTRODUCTION

The following chapter (with the exception of the thesis overview section) was submitted as a review article entitled *Mechanically-mediated adaption to the quality and quantity of bone*. Authors on the paper are Alycia G. Berman (first author) and Joseph M. Wallace (corresponding author). The paper is currently under review. Note that figures have been removed due to copyright restrictions.

1.1 Abstract

Prevention of fracture through improved bone mechanical strength is of great importance given the large number of bone disease-related fractures each year, the decreased quality of life associated with fractures, and the large anticipated increase in fracture incidence over the upcoming years due to the aging population. Exercise and other forms of mechanical stimulation have been shown to increase bone mass, suggesting improved strength. However, while bone mass is a good indicator of strength, other components (such as bone quality) also contribute to bone mechanical integrity. While increased bone mass has been explored considerably using both exercise and targeted loading models, the role of mechanical stimulation in altering bone quality has been explored to a lesser degree. Understanding how to improve both the quantity and quality of bone is critical to increasing fracture resistance. Herein, we discuss quantity and quality-based improvements that have been observed using both exercise and targeted loading models of bone adaptation.

1.2 Introduction

Throughout the course of a lifetime, a persons bones are constantly loaded and unloaded, whether that be through walking, running, bending over, standing up, etc. As is true for any structure and material, the constant fatigue of bone can cause accrual of damage, leading to weakened bone. In order for bone to maintain its mechanical integrity, it must be a dynamic structure, one that is able to repair itself and to adapt to the loads engendered on it.

1.3 Historical Perspective and Clinical Significance

This concept that bone responds to mechanical stimulation is not new. Although Julius Wolff is often credited with the idea (commonly referred to as Wolff's Law due to his 1870 publication [1]), the notion that mechanical loads influence the structure and organization of bone was observed well before, back to at least the 1830s. In 1917, in a book entitled "The Laws of Bone Architecture" [2], the author Koch noted that, in the 1830s, there were three doctors (Bourguery, Ward, and Wyman) whom each described their observations regarding trabecular organization. According to Koch, their observations were rather simplistic, and so perhaps, the true credit for the concept should be given to Georg Hermann von Meyer [3] who connected the dots and wrote a seminal work in 1867 on the idea that trabeculae are arranged in a specific manner which tended to align with the principal stress trajectories in bone. Hermann von Meyer was later followed by Karl Culmann, a mathematician who noted that the alignment of trabecular bone tended to follow a mathematical pattern seen in "graphic statics." In the late 1800s, Wolff referenced von Meyer's and Culmann's works in the creation of his paper, where he discussed the adaptation of trabeculae to load, which eventually came to be known as Wolff's law and is often used as the key reference for the mechanical adaptability of bone.

Effectively, Wolff's law states that bone will adapt to the loads engendered on it. In other words, the trabecular structure of bone is precisely arranged to place

bone where it is needed and remove bone that is not needed in order to maintain structural integrity. Over a hundred years later, in 1987, Harold Frost [4] published a conceptual model on bone adaptation, called The Mechanostat, in which bone itself was seen as a negative feedback system that would respond with either formation or resorption, depending on the local strain field.

This response of bone to mechanical stimulation has been observed in many human exercise studies [5]. A common example is found in tennis players who, due to the forces of impact and muscle loading, often have increased bone mineral content in their dominant arm as compared to their non-dominant arm, as shown in Fig. 1 [6]. Running [7–9], jumping [10], gymnastics [11, 12], weight lifting [13], and swimming [14, 15] have all been shown to increase bone mass as compared to sedentary controls. This bone mass response seems to be dependent on the degree to which the activity is weight bearing [16, 17], as well as the starting age, with pre-menarche women having the greatest increase in bone mineral content [18].

Just as mechanical stimulation can increase bone mass, a decrease in mechanical stimulation (through disease or disuse) can cause a relatively rapid decrease in mass. This decrease can be seen as the bone trying to balance the need for strength with the metabolic costs associated with maintaining that strength. Bone is a dense structure in comparison to other tissues (nearly double the mass per unit volume) and has large metabolic needs. In situations of disuse, bone loss will occur quickly because the body no longer needs to metabolically support such a large structure for load bearing ability [19]. A common example is astronauts, who often experience bone loss due to microgravity while in space [20–23]. In a study of long-duration flights (average duration approximately 6 months), almost all long-duration astronauts experienced at least a 3% bone loss in at least one skeletal site, while 43% showed at least a 10% bone loss in at least one skeletal site [24]. In fact, the decrease in bone in astronauts was found to be approximately 1-1.5% per month [25], and was shown to be up to 2.7% per month in the trabecular region of the femoral neck [26]. Astronauts are not the only ones affected. Bedrest is often used as a model of space flight [24], as it has

been shown to decrease bone density by approximately 0.3-1% per month [27, 28]. In addition, diseases such as osteoporosis are thought to be caused, at least in part, by a failure of bone cells to respond to mechanical stimulation [29]. This bone loss (through space flight, bed rest, osteoporosis, or another mechanism) decreases the body's ability to bear load and can lead to fracture in instances of high impact loading (such as falling).

Prevention of fracture through improved bone mechanical strength is of great importance given the large number of bone disease-related fractures each year, the decreased quality of life associated with fractures, and the large anticipated increase in fracture incidence over the upcoming years due to the aging population [30]. For this reason, much research has been dedicated to understanding how and why bone responds to mechanical load. In addition to clinical studies, the use of pre-clinical animal models has aided greatly in advancing our knowledge on the response of bone to mechanical stimulation.

1.4 Animal Models of Mechanical Stimulation

While clinical studies have provided clear indications that bone adapts to mechanical stimulation, most of our understanding of the specifics of how and why bone adaptation occurs have been derived from studies using pre-clinical animal models. In general, *in vivo* animal models of mechanical adaptation can be divided into two broad groups: intrinsic (i.e. exercise) and extrinsic (i.e. targeted loading).

Exercise, as the name would suggest, refers to loading modalities such as treadmill running [31, 32], jumping [33], swimming [34, 35], and climbing [36, 37]. Exercise models tend to be non-invasive, where loading of bone is delivered through muscle contraction and ground reaction forces. In exercise models, the entire animal is affected which makes these models physiologically relevant. The main limitation, however, is the incomplete control over the mechanical inputs to the bone, which can be dependent on each individual animals activity and activity level, body weight,

etc. It is also difficult to isolate the influences of mechanical loading from those that result from the whole body response.

In contrast, targeted loading provides an alternative means of assessment in that a known load or strain stimulus can be applied to all animals in a consistent manner. A variety of targeted loading models are displayed in Fig. 2. Often, a single limb or single bone is mechanically stimulated. Importantly for the continued use of these models, adaptation of both cortical and cancellous bone has been shown to be confined to the loaded limb and, lacking a systemic effect [38], enables the animal's contralateral limb to act as an internal, non-loaded control. Examples of targeted loading include the use of surgical pins [39], four-point bending [40], cantilever tibial loading [41], ulnar loading [42, 43], and tibial loading [44].

1.4.1 Extrinsic Factors Influencing Bone Formation Response

Both exercise and targeted loading have significantly advanced our understanding of what triggers a bone formation response. For example, the strain stimulus during loading must be above a certain threshold [45] and the loading must be dynamic (not static) [46] in order for bone to respond. The threshold was later found to be location dependent, and it was demonstrated in the rat ulna that the threshold strain was higher in areas that were regularly subjected to larger in vivo mechanical strains [47]. Once above that strain, bone formation responds linearly to the amount of strain engendered [45, 48]. Strain rate also has an impact, with high strain rates resulting in higher bone formation rates while static loads had no effect [46, 49, 50]. Inserting rest into the loading bouts also increases the bone formation response [51–53], and is thought to involve the modulation of intracellular levels of calcium in osteoblasts, better allowing them to respond to load [54].

Most of the initial bone adaptation studies focused exclusively on cortical adaptation, since many of the early targeted loading models were unable to be used to assess cancellous bone. However, with the addition of the ulnar and tibial loading

models, the response of cancellous bone could also be probed [44]. Cancellous bone adaptation has been observed in both male and female mice [55], with a response even more robust than was observed in cortical bone [56]. This response in cancellous regions has implications for osteoporosis since cancellous regions are often at greatest risk for fracture [56].

In both cortical and cancellous regions, the strain engendered on bone plays an integral role in determining its adaptive response. For that reason, the addition of finite element analysis models has been crucial in enabling us to understand the strain field engendered on bone for the various animal loading modalities. Numerous studies have explored strain distributions under the loading regimes, each involving increasingly more sophisticated models [57–61]. Digital image correlation (DIC) has also been used to assess surface strains experimentally. For example, Sztefek et al. measured surface strain using DIC and reported that after tibial loading, the surface strains were reduced and more uniform than before loading [62], suggesting that bone responds to mechanical stimulation as a means of reducing strain.

1.4.2 Intrinsic Factors Influencing Bone Formation Response

As our understanding of bone adaptation has increased, research in this area has expanded to also include an assessment of various intrinsic factors with the aim of understanding what causes bone to respond as it does.

The use of genetic animal models has been beneficial, both as a way to understand why some humans might show a better response to loading than others, as well as a means of exploring cellular pathways related to the response. For example, bone adaptation occurs more readily in models of low density bone (C57BL/6J mice) as compared to models of high density bone (C3H/HeJ mice) using targeted tibial loading [63]. Similarly, a genetic study exploring three mouse strains (C3H/He, C57BL/6, and DBA/2) showed decreased responsiveness in the C3H/He mice [64]. Together, these studies suggest that genetics contribute to a person's predisposition

for high or low bone mass and may also impact their ability to adapt to mechanical stimulation. Genetic mouse models have also been used to tease out some of the underlying molecular pathways involved in the loading response. LRP5-deficient mice were used and showed that the LRP5 mutation was associated with increased response to loading [65], while sclerostin-deficient mice demonstrated that long-term sclerostin deficiency can result in increased bone formation [66].

Another major area of exploration has focused on the influence of age. At 26 weeks of age, skeletally mature mice showed reduced sensitivity to mechanical stimulation as compared to actively growing 10 week old mice, even though both young and old mice responded to load. It was suggested that this effect was driven by a decrease in bone tissue deformation [67]. Interestingly, in another study, the strains engendered on bone increased with age due to cortical thinning as assessed experimentally and with a finite element model [58]. This disparity might be driven by the fact that the second study used mice at 5, 12 and 22 months of age, versus at 2.5 and 6 months of age as was the case in the first study. In another study that explored the role of loading in young and old mice at either the same strain level or the same load level, it was found that the same load level (which was a higher strain level) was required in the old mice to observe an adaptive effect [68].

As we continue to explore the effects of intrinsic factors (such as age and genetics), we can begin to tease out some of the reasons for the biological variability observed by understanding the role of various factors on bone adaptation.

1.4.3 Mechanical Stimulation in Pre-clinical Assessment

The use of animal disease models has enabled pre-clinical assessment of the effect of loading in the context of disease. For example, tibial loading was able to prevent bone loss after orchidectomy [69]. In addition, there has been an increase in the exploration of combination treatments, through which it has been observed that

loading can synergistically improve the effect of drug treatments such as parathyroid hormone [70] and tamoxifen [71], but not fulvestrant [71].

These studies, and more, have profoundly impacted our understanding of mechanical stimulation. However, as will be discussed in the next section, we must be careful to not confuse improved bone mass with decreased fracture risk.

1.5 Quality Versus Quantity

Much of the focus of the above studies has been in understanding what triggers a bone formation response, with outcomes typically restricted to bone formation rate, bone mass, and bone mineral density. While these studies have been beneficial in increasing our understanding of what drives bone formation, they beg the question as to the importance of increased bone mass in relation to decreased fracture risk. For example, while BMD is a good predictor of fracture risk, other components of bone strength make it difficult for BMD alone to assess fracture [72, 73]. Thus, if the ultimate goal is to decrease fracture risk in patients with compromised bone structure, we must be sure that the treatments (exercise, targeted loading, etc.) not only positively impact bone mass, but also bone mechanical integrity. If we are merely increasing bone mass without improving mechanical integrity, we are not achieving our end goal.

While bone mass alone should not be the end all assessment to reduce fracture, increased bone mass is still a good outcome. This makes intuitive sense since something that is larger usually requires a greater force to break. Take, for example, a pencil and a tree branch. Both may be made from the same wood, but experience informs us that the pencil will be easier to break. For bone, similar principles apply. In terms of mechanics, a greater cross-sectional area will decrease tissue-level stress (the force experienced by the tissue itself) by distributing a given force over more material and thus, decreases the risk of fracture. However, as mentioned previously, bone mineral density and bone mass incompletely predict fracture risk, suggesting

that there is more to the story. Often, this unknown contributor to bone strength is referred to by the ill-defined term bone quality.

Bone quality, in essence, is the ability of the bone tissue itself to resist load, without regard for its mass and structural morphology. It can be related to the inherent states of the two primary components of the bone matrix: hydroxyapatite and Type I collagen. Some measurable contributors to bone quality include chemical composition, degree of collagen cross-linking, accumulation of advanced glycation end-products (AGEs), microdamage, mineral-matrix interactions, and collagen fiber orientation [74–77]. All of these factors can influence toughening mechanisms in bone [78], thus altering its ability to bear load and absorb energy. Some bone diseases result in increased fracture risk due to decreased bone quality. Take, for example, diabetes. Although diabetic patients often have average or increased BMD, they are also considered to be at higher risk of fracture due to the decreased quality of their tissue, generally attributed to an accumulation of AGEs [79].

Thus, an important question to ask regarding bone adaptation to mechanical load is, how are bone quality and tissue-level properties affected?

1.6 Mechanical Stimulation and Bone Quality

In answer to this, recent research has begun to focus on understanding the contributors of bone tissue quality and how they are affected by mechanical loading. Many of the studies show promising effects with respect to the ability of mechanical stimulation to improve bone quality.

An interesting example of the quality/quantity conundrum has been shown in swimming rats. Although clinical and pre-clinical studies have suggested that non-load bearing activities such as swimming only result in mild increases (and sometimes even decreases) in bone mineral content and bone mass [80–82], the post-yield mechanical properties of bones from swimming rats were significantly increased as compared to their sedentary controls [83]. Improved post-yield parameters are im-

portant in that they can be related to a bones ability to resist catastrophic failure by dissipating energy through damage accrual. This damage can later be repaired through targeted remodeling. Given the effect on post-yield mechanical properties, the results were attributed to modifications in collagen since post-yield behavior is most often associated with the state of collagen in bone. In support of the ability of exercise to alter collagen, Isaksson et al. demonstrated that following voluntary running in mice, mechanical properties of the bone collagen network were significantly increased [84]. These benefits came without any changes in collagen content, indicating loading-induced improvements to the collagen network itself.

An increase in post-yield parameters has also been observed in treadmill exercised mice in which, after three weeks of running, mice exhibited increased post-yield mechanical behavior as compared to sedentary controls even though there was no change in bone size or shape [31]. These findings suggested that changes in bone quality, and specifically in collagen, were responsible. Interestingly, when mice were subjected to this running protocol for 3 weeks and then allowed 2 additional weeks of latency, the post-yield benefits of exercise were maintained while tissue stiffness and strength increased [85]. These changes, which continued after the termination of loading, suggested that the modifications to collagen may require time to mature; hence, the increased strength with the latency period.

Beyond impacts on monotonic mechanical properties, exercise and loading have other effects which can also be related to changes in bone quality. These include effects on fatigue life or the ability of bone to accrue and tolerate damage due to repeated loading in the absence of a repair mechanism (*ex vivo*). One such study of modified fatigue life involved the rat ulnar loading model [86]. Warden, et al. loaded the ulna of rats daily for 7 weeks followed by 92 weeks of detraining to assess changes in bone quality induced by loading as well as the ability to maintain those changes over time. Although BMC values measured using DXA were the same in the loaded and non-loaded limbs after detraining, the structure (minimum moment of inertia) was larger in the loaded group and the fatigue life was significantly increased

compared with controls. There were also increases in whole bone (ash content) and localized (phosphate-to-protein) mineralization, as well as in the carbonate to protein ratio in the loaded ulnas. Consistent with the increase in mineralization, the exercised ulnas had increased stiffness and strength, but decreased post-yield behavior, suggesting a more brittle bone. However, despite the increase in brittleness, the increase in fatigue life suggests that the bone was still better able to resist fatigue loading-induced failure, likely through modification in the bones organic phase (i.e. collagen).

A loading-induced improvement in fatigue life was also observed in a study by Kohn, et al. [87]. Using 16-week old male mice, 3 weeks of treadmill running significantly improved tissue strength and fatigue resistance without changes in bone size. Specifically, tibiae from control and exercised mice had similar levels of microcracks and diffuse damage. However, the number of new cracks formed during ex vivo fatigue loading was lessened in exercised bones, suggesting that exercise made the bones more resistant to damage accrual during fatigue. In sedentary mice, fatigue loading altered the mineral-matrix ratio and increased the disorder of the secondary structure of collagen in bone. These results were not observed in exercised mice, indicating that the exercised bones were better able to resist damage to the collagen matrix. Given the lack of changes in bone size (similar to what was seen in the ulnar loading study above, [86]), these results all suggest a direct effect of loading on bone tissue quality, potentially due to changes in collagen specifically.

Although studies of mechanical stimulation on bone quality have shown promising results, not all effects have been positive. Mosekilde, et al. [88] showed that 6 months of treadmill running in rats resulted in increased BV/TV and increased cross-sectional area, but no mechanical improvements in the vertebrae. In addition, the femoral midshaft had increased cortical thickness, but no change in ash content, collagen content, apparent density, or mechanical properties. Some of this seeming disparity in results might be driven by the difference in pre-yield and post-yield parameters. Namely, many of the positive effects of loading noted in the above para-

graphs have been in either post-yield properties or fatigue parameters, neither of which were addressed in this study. The discussion of pre- and post-yield properties raises another concern. Although many have demonstrated increases in post-yield parameters, those increases are often accompanied by decreases in pre-yield mechanical properties [31, 83]. The decrease in pre-yield mechanical properties could be ameliorated by an additional period of latency [85]. However, the reason for this alteration and the role that pre-yield and post-yield parameters play in ultimately determining fracture resistance remains to be elucidated. Altogether, although many of the studies show positive quality-based effects of mechanical stimulation, not all studies do, and due to the paucity of information on this topic, the reasons for these discrepancies are not clear.

1.7 Conclusion

Mechanical stimulation (whether through exercise or targeted loading modalities) has been shown to beneficially affect bone mass. However, we must be certain that these effects also contribute to improved bone quality and ultimately, to decreased fracture risk. Recent studies have shown mostly positive results, suggesting that loading may cause quality-based changes in bone. However, there have also been several studies that show opposite trends. For that reason, future research is needed to assess specific components of loading that may either contribute to or prevent quality-based improvements to bone so that ultimately, an understanding of how to improve both quantity and quality can be achieved.

1.8 Thesis Overview

As discussed in the above sections, although bone quality is important, our understanding of how mechanical stimulation impacts collagen quality is limited. With this in mind, this thesis focuses on understanding how mechanical stimuli protect the formation of bone, leading to improved bone quality.

In Chapters 2 and 3, this area was explored through use of a diseased mouse model (osteolathyrism, induced by injection of β -aminopropionitrile (BAPN)). BAPN causes a collagen quality-based disease by disrupting the formation and maturation of enzymatic cross-links. Targeted tibial loading was then employed as a means of assessing how the body is able to respond and compensate for decreased bone quality. Specific to Chapter 2, a low dose of BAPN was injected which was unable to induce an effect. For that reason, in Chapter 3, a high dose of BAPN was used. Unfortunately, even the high dose was unable to induce a functional disease.

Although Chapters 2 and 3 were unable to demonstrate a functional disease, the results of the two studies suggested that the difference between quantity-based and quality-based improvements to bone through loading may be, to some degree, dependent on the amount of injury. For that reason, in Chapter 4, control mice were loaded under various regimes and various pain parameters were observed to determine how to decrease mouse injury during loading, in an effort to increase quality, and not just quantity, of bone produced.

Lastly, in Chapter 5, a summary of results are discussed and potential future directions are explored.

1.9 References

- [1] J. Wolff, "Ueber die innere architectur der knochen und ihre bedeutung fr die frage vom knochenwachsthum," *Archiv fr pathologische Anatomie und Physiologie und fr klinische Medicin*, vol. 50, no. 3, pp. 389–450, 1870.
- [2] J. Koch, "The laws of bone architecture," *American Journal of Anatomy*, vol. 21, no. 177, 1917.
- [3] G. Meyer, "Die architektur der spongiosa, archief fur den anatomischen und physiologischen," *Wissenschaften im Medicin*, vol. 27, no. 4, pp. 1389–1394, 1867.
- [4] H. Frost, "The mechanostat: a proposed pathogenetic mechanism of osteoporoses and the bone mass effects of mechanical and nonmechanical agents," *Bone and Mineral*, vol. 2, no. 2, 1987.
- [5] G. A. Kelley and K. S. Kelley, "Exercise and bone mineral density at the femoral neck in postmenopausal women: A meta-analysis of controlled clinical trials with individual patient data," *American Journal of Obstetrics and Gynecology*, vol. 194, no. 3, pp. 760–767, 2006. [Online]. Available: <http://www.sciencedirect.com/science/article/pii/S0002937805014626>
- [6] A. L. Huddleston, D. Rockwell, D. N. Kulund, and R. B. Harrison, "Bone mass in lifetime tennis athletes," *JAMA*, vol. 244, no. 10, pp. 1107–9, 1980. [Online]. Available: <http://www.ncbi.nlm.nih.gov/pubmed/7411762>
- [7] N. Dalen and K. E. Olsson, "Bone mineral content and physical activity," *Acta Orthop Scand*, vol. 45, no. 2, pp. 170–4, 1974. [Online]. Available: <http://www.ncbi.nlm.nih.gov/pubmed/4406972>
- [8] R. L. Wolman, L. Faulmann, P. Clark, R. Hesp, and M. G. Harries, "Different training patterns and bone mineral density of the femoral shaft in elite, female athletes," *Ann Rheum Dis*, vol. 50, no. 7, pp. 487–9, 1991. [Online]. Available: <http://www.ncbi.nlm.nih.gov/pubmed/1877854>
- [9] V. Brewer, B. M. Meyer, M. S. Keele, S. J. Upton, and R. D. Hagan, "Role of exercise in prevention of involutinal bone loss," *Med Sci Sports Exerc*, vol. 15, no. 6, pp. 445–9, 1983. [Online]. Available: <http://www.ncbi.nlm.nih.gov/pubmed/6656552>
- [10] R. K. Fuchs, J. J. Bauer, and C. M. Snow, "Jumping improves hip and lumbar spine bone mass in prepubescent children: a randomized controlled trial," *J Bone Miner Res*, vol. 16, no. 1, pp. 148–56, 2001. [Online]. Available: <http://www.ncbi.nlm.nih.gov/pubmed/11149479>
- [11] E. M. Kirchner, R. D. Lewis, and P. J. O'Connor, "Effect of past gymnastics participation on adult bone mass," *J Appl Physiol (1985)*, vol. 80, no. 1, pp. 226–32, 1996. [Online]. Available: <http://www.ncbi.nlm.nih.gov/pubmed/8847307>
- [12] C. M. Snow, D. P. Williams, J. LaRiviere, R. K. Fuchs, and T. L. Robinson, "Bone gains and losses follow seasonal training and detraining in gymnasts," *Calcif Tissue Int*, vol. 69, no. 1, pp. 7–12, 2001. [Online]. Available: <http://www.ncbi.nlm.nih.gov/pubmed/11685427>

- [13] L. A. Colletti, J. Edwards, L. Gordon, J. Shary, and N. H. Bell, "The effects of muscle-building exercise on bone mineral density of the radius, spine, and hip in young men," *Calcif Tissue Int*, vol. 45, no. 1, pp. 12–4, 1989. [Online]. Available: <http://www.ncbi.nlm.nih.gov/pubmed/2504457>
- [14] P. C. Jacobson, W. Beaver, S. A. Grubb, T. N. Taft, and R. V. Talmage, "Bone density in women: college athletes and older athletic women," *J Orthop Res*, vol. 2, no. 4, pp. 328–32, 1984. [Online]. Available: <http://www.ncbi.nlm.nih.gov/pubmed/6335524>
- [15] E. S. Orwoll, J. Ferar, S. K. Oviatt, M. R. McClung, and K. Huntington, "The relationship of swimming exercise to bone mass in men and women," *Arch Intern Med*, vol. 149, no. 10, pp. 2197–200, 1989. [Online]. Available: <http://www.ncbi.nlm.nih.gov/pubmed/2802886>
- [16] D. Courteix, E. Lespessailles, S. L. Peres, P. Obert, P. Germain, and C. L. Benhamou, "Effect of physical training on bone mineral density in prepubertal girls: a comparative study between impact-loading and non-impact-loading sports," *Osteoporos Int*, vol. 8, no. 2, pp. 152–8, 1998. [Online]. Available: <http://www.ncbi.nlm.nih.gov/pubmed/9666939>
- [17] C. S. Duncan, C. J. Blimkie, C. T. Cowell, S. T. Burke, J. N. Briody, and R. Howman-Giles, "Bone mineral density in adolescent female athletes: relationship to exercise type and muscle strength," *Med Sci Sports Exerc*, vol. 34, no. 2, pp. 286–94, 2002. [Online]. Available: <http://www.ncbi.nlm.nih.gov/pubmed/11828239>
- [18] P. Kannus, H. Haapasalo, M. Sankelo, H. Sievanen, M. Pasanen, A. Heinonen, P. Oja, and I. Vuori, "Effect of starting age of physical activity on bone mass in the dominant arm of tennis and squash players," *Ann Intern Med*, vol. 123, no. 1, pp. 27–31, 1995. [Online]. Available: <http://www.ncbi.nlm.nih.gov/pubmed/7762910>
- [19] J. D. Currey, *Bones: structure and mechanics*. Princeton university press, 2002.
- [20] D. Grimm, J. Grosse, M. Wehland, V. Mann, J. E. Reseland, A. Sundaresan, and T. J. Corydon, "The impact of microgravity on bone in humans," *Bone*, vol. 87, pp. 44–56, 2016. [Online]. Available: <http://www.ncbi.nlm.nih.gov/pubmed/27032715>
- [21] E. S. Orwoll, R. A. Adler, S. Amin, N. Binkley, E. M. Lewiecki, S. M. Petak, S. A. Shapses, M. Sinaki, N. B. Watts, and J. D. Sibonga, "Skeletal health in long-duration astronauts: nature, assessment, and management recommendations from the nasa bone summit," *J Bone Miner Res*, vol. 28, no. 6, pp. 1243–55, 2013. [Online]. Available: <http://www.ncbi.nlm.nih.gov/pubmed/23553962>
- [22] J. D. Sibonga, P. R. Cavanagh, T. F. Lang, A. D. LeBlanc, V. S. Schneider, L. C. Shackelford, S. M. Smith, and L. Vico, "Adaptation of the skeletal system during long-duration spaceflight," *Clinical Reviews in Bone and Mineral Metabolism*, vol. 5, no. 4, pp. 249–261, 2007. [Online]. Available: <http://dx.doi.org/10.1007/s12018-008-9012-8>

- [23] S. M. Smith, S. R. Zwart, M. Heer, E. K. Hudson, L. Shackelford, and J. L. Morgan, "Men and women in space: bone loss and kidney stone risk after long-duration spaceflight," *J Bone Miner Res*, vol. 29, no. 7, pp. 1639–45, 2014. [Online]. Available: <http://www.ncbi.nlm.nih.gov/pubmed/24470067>
- [24] A. D. LeBlanc, E. R. Spector, H. J. Evans, and J. D. Sibonga, "Skeletal responses to space flight and the bed rest analog: a review," *J Musculoskeletal Neuronal Interact*, vol. 7, no. 1, pp. 33–47, 2007. [Online]. Available: <http://www.ncbi.nlm.nih.gov/pubmed/17396004>
- [25] A. LeBlanc, V. Schneider, L. Shackelford, S. West, V. Oganov, A. Bakulin, and L. Voronin, "Bone mineral and lean tissue loss after long duration space flight," *J Musculoskeletal Neuronal Interact*, vol. 1, no. 2, pp. 157–60, 2000. [Online]. Available: <http://www.ncbi.nlm.nih.gov/pubmed/15758512>
- [26] T. Lang, A. LeBlanc, H. Evans, Y. Lu, H. Genant, and A. Yu, "Cortical and trabecular bone mineral loss from the spine and hip in long-duration spaceflight," *J Bone Miner Res*, vol. 19, no. 6, pp. 1006–12, 2004. [Online]. Available: <http://www.ncbi.nlm.nih.gov/pubmed/15125798>
- [27] A. Pavy-Le Traon, M. Heer, M. V. Narici, J. Rittweger, and J. Vernikos, "From space to earth: advances in human physiology from 20 years of bed rest studies (1986-2006)," *Eur J Appl Physiol*, vol. 101, no. 2, pp. 143–94, 2007. [Online]. Available: <http://www.ncbi.nlm.nih.gov/pubmed/17661073>
- [28] A. R. Hargens and L. Vico, "Long-duration bed rest as an analog to microgravity," *Journal of Applied Physiology*, vol. 120, no. 8, pp. 891–903, 2016. [Online]. Available: <http://jap.physiology.org/content/120/8/891.abstract>
- [29] L. Lanyon and T. Skerry, "Perspective: Postmenopausal osteoporosis as a failure of bone's adaptation to functional loading: A hypothesis*," *Journal of Bone and Mineral Research*, vol. 16, no. 11, pp. 1937–1947, 2001. [Online]. Available: <http://dx.doi.org/10.1359/jbmr.2001.16.11.1937>
- [30] ser. Reports of the Surgeon General, Rockville (MD), 2004. [Online]. Available: <http://www.ncbi.nlm.nih.gov/pubmed/20945569>
- [31] J. M. Wallace, R. M. Rajachar, M. R. Allen, S. A. Bloomfield, P. G. Robey, M. F. Young, and D. H. Kohn, "Exercise-induced changes in the cortical bone of growing mice are bone and gender specific," *Bone*, vol. 40, no. 4, pp. 1120–1127, 2007. [Online]. Available: <http://www.ncbi.nlm.nih.gov/pmc/articles/PMC2729655/>
- [32] J. Iwamoto, J. K. Yeh, and J. F. Aloia, "Differential effect of treadmill exercise on three cancellous bone sites in the young growing rat," *Bone*, vol. 24, no. 3, pp. 163–169, 1999. [Online]. Available: <http://www.sciencedirect.com/science/article/pii/S8756328298001896>
- [33] Y. Umemura, T. Ishiko, T. Yamauchi, M. Kuroono, and S. Mashiko, "Five jumps per day increase bone mass and breaking force in rats," *Journal of Bone and Mineral Research*, vol. 12, no. 9, pp. 1480–1485, 1997. [Online]. Available: <http://dx.doi.org/10.1359/jbmr.1997.12.9.1480>

- [34] T. H. Huang, S. C. Lin, F. L. Chang, S. S. Hsieh, S. H. Liu, and R. S. Yang, "Effects of different exercise modes on mineralization, structure, and biomechanical properties of growing bone," *Journal of Applied Physiology*, vol. 95, no. 1, pp. 300–307, 2003. [Online]. Available: <http://jap.physiology.org/content/jap/95/1/300.full.pdf>
- [35] K. J. Hart, J. M. Shaw, E. Vajda, M. Hegsted, and S. C. Miller, "Swim-trained rats have greater bone mass, density, strength, and dynamics," *Journal of Applied Physiology*, vol. 91, no. 4, pp. 1663–1668, 2001. [Online]. Available: <http://jap.physiology.org/content/jap/91/4/1663.full.pdf>
- [36] T. Notomi, N. Okimoto, Y. Okazaki, Y. Tanaka, T. Nakamura, and M. Suzuki, "Effects of tower climbing exercise on bone mass, strength, and turnover in growing rats," *Journal of Bone and Mineral Research*, vol. 16, no. 1, pp. 166–174, 2001. [Online]. Available: <http://dx.doi.org/10.1359/jbmr.2001.16.1.166>
- [37] T. Mori, N. Okimoto, A. Sakai, Y. Okazaki, N. Nakura, T. Notomi, and T. Nakamura, "Climbing exercise increases bone mass and trabecular bone turnover through transient regulation of marrow osteogenic and osteoclastogenic potentials in mice," *Journal of Bone and Mineral Research*, vol. 18, no. 11, pp. 2002–2009, 2003. [Online]. Available: <http://dx.doi.org/10.1359/jbmr.2003.18.11.2002>
- [38] T. Sugiyama, J. S. Price, and L. E. Lanyon, "Functional adaptation to mechanical loading in both cortical and cancellous bone is controlled locally and is confined to the loaded bones," *Bone*, vol. 46, no. 2, pp. 314–321, 2010. [Online]. Available: <http://www.sciencedirect.com/science/article/pii/S8756328209018845>
- [39] C. T. Rubin and L. Lanyon, "Regulation of bone formation by applied dynamic loads," *The Journal of Bone & Joint Surgery*, vol. 66, no. 3, pp. 397–402, 1984.
- [40] C. H. Turner, M. P. Akhter, D. M. Raab, D. B. Kimmel, and R. R. Recker, "A noninvasive, in vivo model for studying strain adaptive bone modeling," *Bone*, vol. 12, no. 2, pp. 73–79, 1991. [Online]. Available: <http://www.sciencedirect.com/science/article/pii/8756328291900032>
- [41] T. S. Gross, S. Srinivasan, C. C. Liu, T. L. Clemens, and S. D. Bain, "Noninvasive loading of the murine tibia: An in vivo model for the study of mechanotransduction," *Journal of Bone and Mineral Research*, vol. 17, no. 3, pp. 493–501, 2002. [Online]. Available: <http://dx.doi.org/10.1359/jbmr.2002.17.3.493>
- [42] A. G. Torrance, J. R. Mosley, R. F. Suswillo, and L. E. Lanyon, "Noninvasive loading of the rat ulna in vivo induces a strain-related modeling response uncomplicated by trauma or periosteal pressure," *Calcif Tissue Int*, vol. 54, no. 3, pp. 241–7, 1994. [Online]. Available: <http://www.ncbi.nlm.nih.gov/pubmed/8055374>
- [43] K. C. Lee, A. Maxwell, and L. E. Lanyon, "Validation of a technique for studying functional adaptation of the mouse ulna in response to mechanical loading," *Bone*, vol. 31, no. 3, pp. 407–12, 2002. [Online]. Available: <http://www.ncbi.nlm.nih.gov/pubmed/12231414>

- [44] R. L. De Souza, M. Matsuura, F. Eckstein, S. C. F. Rawlinson, L. E. Lanyon, and A. A. Pitsillides, "Non-invasive axial loading of mouse tibiae increases cortical bone formation and modifies trabecular organization: A new model to study cortical and cancellous compartments in a single loaded element," *Bone*, vol. 37, no. 6, pp. 810–818. [Online]. Available: <http://dx.doi.org/10.1016/j.bone.2005.07.022>
- [45] C. H. Turner, M. R. Forwood, J. Y. Rho, and T. Yoshikawa, "Mechanical loading thresholds for lamellar and woven bone formation," *Journal of Bone and Mineral Research*, vol. 9, no. 1, pp. 87–97, 1994. [Online]. Available: <http://dx.doi.org/10.1002/jbmr.5650090113>
- [46] C. H. Turner, I. Owan, and Y. Takano, "Mechanotransduction in bone: role of strain rate," *American Journal of Physiology - Endocrinology and Metabolism*, vol. 269, no. 3, pp. E438–E442, 1995. [Online]. Available: <http://ajpendo.physiology.org/content/ajpendo/269/3/E438.full.pdf>
- [47] Y.-F. Hsieh, A. G. Robling, W. T. Ambrosius, D. B. Burr, and C. H. Turner, "Mechanical loading of diaphyseal bone in vivo: The strain threshold for an osteogenic response varies with location," *Journal of Bone and Mineral Research*, vol. 16, no. 12, pp. 2291–2297, 2001. [Online]. Available: <http://dx.doi.org/10.1359/jbmr.2001.16.12.2291>
- [48] C. T. Rubin and L. E. Lanyon, "Regulation of bone mass by mechanical strain magnitude," *Calcified Tissue International*, vol. 37, no. 4, pp. 411–417, 1985. [Online]. Available: <http://dx.doi.org/10.1007/BF02553711>
- [49] Y.-F. Hsieh and C. H. Turner, "Effects of loading frequency on mechanically induced bone formation," *Journal of Bone and Mineral Research*, vol. 16, no. 5, pp. 918–924, 2001. [Online]. Available: <http://dx.doi.org/10.1359/jbmr.2001.16.5.918>
- [50] J. R. Mosley and L. E. Lanyon, "Strain rate as a controlling influence on adaptive modeling in response to dynamic loading of the ulna in growing male rats," *Bone*, vol. 23, no. 4, pp. 313–318, 1998. [Online]. Available: <http://www.sciencedirect.com/science/article/pii/S8756328298001136>
- [51] A. G. Robling, F. M. Hinant, D. B. Burr, and C. H. Turner, "Improved bone structure and strength after long-term mechanical loading is greatest if loading is separated into short bouts," *Journal of Bone and Mineral Research*, vol. 17, no. 8, pp. 1545–1554, 2002. [Online]. Available: <http://dx.doi.org/10.1359/jbmr.2002.17.8.1545>
- [52] S. Srinivasan, D. A. Weimer, S. C. Agans, S. D. Bain, and T. S. Gross, "Low-magnitude mechanical loading becomes osteogenic when rest is inserted between each load cycle," *Journal of Bone and Mineral Research*, vol. 17, no. 9, pp. 1613–1620, 2002. [Online]. Available: <http://dx.doi.org/10.1359/jbmr.2002.17.9.1613>
- [53] A. G. Robling, D. B. Burr, and C. H. Turner, "Recovery periods restore mechanosensitivity to dynamically loaded bone," *Journal of Experimental Biology*, vol. 204, no. 19, pp. 3389–3399, 2001. [Online]. Available: <http://jeb.biologists.org/content/jexbio/204/19/3389.full.pdf>

- [54] N. N. Batra, Y. J. Li, C. E. Yellowley, L. You, A. M. Malone, C. H. Kim, and C. R. Jacobs, "Effects of short-term recovery periods on fluid-induced signaling in osteoblastic cells," *Journal of Biomechanics*, vol. 38, no. 9, pp. 1909–1917. [Online]. Available: <http://dx.doi.org/10.1016/j.jbiomech.2004.08.009>
- [55] M. E. Lynch, R. P. Main, Q. Xu, D. J. Walsh, M. B. Schaffler, T. M. Wright, and M. C. H. van der Meulen, "Cancellous bone adaptation to tibial compression is not sex dependent in growing mice," *Journal of Applied Physiology*, vol. 109, no. 3, pp. 685–691, 2010. [Online]. Available: <http://jap.physiology.org/content/jap/109/3/685.full.pdf>
- [56] J. C. Fritton, E. R. Myers, T. M. Wright, and M. C. H. van der Meulen, "Loading induces site-specific increases in mineral content assessed by microcomputed tomography of the mouse tibia," *Bone*, vol. 36, no. 6, pp. 1030–1038, 2005. [Online]. Available: <http://www.sciencedirect.com/science/article/pii/S8756328205000621>
- [57] H. Yang, K. D. Butz, D. Duffy, G. L. Niebur, E. A. Nauman, and R. P. Main, "Characterization of cancellous and cortical bone strain in the in vivo mouse tibial loading model using microct-based finite element analysis," *Bone*, vol. 66, pp. 131–139, 2014. [Online]. Available: <http://www.sciencedirect.com/science/article/pii/S8756328214001963>
- [58] T. K. Patel, M. D. Brodt, and M. J. Silva, "Experimental and finite element analysis of strains induced by axial tibial compression in young-adult and old female c57bl/6 mice," *J Biomech*, vol. 47, no. 2, pp. 451–7, 2014. [Online]. Available: <http://www.ncbi.nlm.nih.gov/pubmed/24268312>
- [59] A. Torcasio, X. Zhang, J. Duyck, and G. H. van Lenthe, "3d characterization of bone strains in the rat tibia loading model," *Biomechanics and Modeling in Mechanobiology*, vol. 11, no. 3, pp. 403–410, 2012. [Online]. Available: <http://dx.doi.org/10.1007/s10237-011-0320-4>
- [60] Y. Lu, G. Thiagarajan, D. P. Nicoletta, and M. L. Johnson, "Load/strain distribution between ulna and radius in the mouse forearm compression loading model," *Medical engineering & physics*, vol. 34, no. 3, pp. 350–356, 2012. [Online]. Available: <http://www.ncbi.nlm.nih.gov/pmc/articles/PMC3251705/>
- [61] M. P. Akhter, D. M. Raab, C. H. Turner, D. B. Kimmel, and R. R. Recker, "Characterization of in vivo strain in the rat tibia during external application of a four-point bending load," *Journal of Biomechanics*, vol. 25, no. 10, pp. 1241–1246, 1992. [Online]. Available: <http://www.sciencedirect.com/science/article/pii/002192909290082C>
- [62] P. Sztfekek, M. Vanleene, R. Olsson, R. Collinson, A. A. Pitsillides, and S. Shefelbine, "Using digital image correlation to determine bone surface strains during loading and after adaptation of the mouse tibia," *Journal of Biomechanics*, vol. 43, no. 4, pp. 599–605, 2010. [Online]. Available: <http://www.sciencedirect.com/science/article/pii/S0021929009006290>
- [63] P. M. Akhter, M. D. Cullen, A. E. Pedersen, B. D. Kimmel, and R. R. Recker, "Bone response to in vivo mechanical loading in two breeds of mice," *Calcified Tissue International*, vol. 63, no. 5, pp. 442–449, 1998. [Online]. Available: <http://dx.doi.org/10.1007/s002239900554>

- [64] A. G. Robling and C. H. Turner, "Mechanotransduction in bone: genetic effects on mechanosensitivity in mice," *Bone*, vol. 31, no. 5, pp. 562–569. [Online]. Available: [http://dx.doi.org/10.1016/S8756-3282\(02\)00871-2](http://dx.doi.org/10.1016/S8756-3282(02)00871-2)
- [65] L. K. Saxon, B. F. Jackson, T. Sugiyama, L. E. Lanyon, and J. S. Price, "Analysis of multiple bone responses to graded strains above functional levels, and to disuse, in mice in vivo show that the human *lrp5* g171v high bone mass mutation increases the osteogenic response to loading but that lack of *lrp5* activity reduces it," *Bone*, vol. 49, no. 2, pp. 184–193, 2011. [Online]. Available: <http://www.sciencedirect.com/science/article/pii/S8756328211007915>
- [66] A. Morse, M. M. McDonald, N. H. Kelly, K. M. Melville, A. Schindeler, I. Kramer, M. Kneissel, M. C. H. van der Meulen, and D. G. Little, "Mechanical load increases in bone formation via a sclerostin-independent pathway," *Journal of Bone and Mineral Research*, vol. 29, no. 11, pp. 2456–2467, 2014. [Online]. Available: <http://dx.doi.org/10.1002/jbmr.2278>
- [67] B. M. Willie, A. I. Birkhold, H. Razi, T. Thiele, M. Aido, B. Kruck, A. Schill, S. Checa, R. P. Main, and G. N. Duda, "Diminished response to in vivo mechanical loading in trabecular and not cortical bone in adulthood of female c57bl/6 mice coincides with a reduction in deformation to load," *Bone*, vol. 55, no. 2, pp. 335–46, 2013. [Online]. Available: <http://www.ncbi.nlm.nih.gov/pubmed/23643681>
- [68] M. E. Lynch, R. P. Main, Q. Xu, T. L. Schmicker, M. B. Schaffler, T. M. Wright, and M. C. H. van der Meulen, "Tibial compression is anabolic in the adult mouse skeleton despite reduced responsiveness with aging," *Bone*, vol. 49, no. 3, pp. 439–446, 2011. [Online]. Available: <http://www.sciencedirect.com/science/article/pii/S8756328211009914>
- [69] J. C. Fritton, E. R. Myers, T. M. Wright, and M. C. H. van der Meulen, "Bone mass is preserved and cancellous architecture altered due to cyclic loading of the mouse tibia after orchidectomy," *Journal of Bone and Mineral Research*, vol. 23, no. 5, pp. 663–671, 2008. [Online]. Available: <http://dx.doi.org/10.1359/jbmr.080104>
- [70] T. Sugiyama, L. K. Saxon, G. Zaman, A. Moustafa, A. Sunter, J. S. Price, and L. E. Lanyon, "Mechanical loading enhances the anabolic effects of intermittent parathyroid hormone (1–34) on trabecular and cortical bone in mice," *Bone*, vol. 43, no. 2, pp. 238–248. [Online]. Available: <http://dx.doi.org/10.1016/j.bone.2008.04.012>
- [71] T. Sugiyama, G. L. Galea, L. E. Lanyon, and J. S. Price, "Mechanical loading-related bone gain is enhanced by tamoxifen but unaffected by fulvestrant in female mice," *Endocrinology*, vol. 151, no. 12, pp. 5582–90, 2010. [Online]. Available: <http://www.ncbi.nlm.nih.gov/pubmed/20943807>
- [72] J. A. Kanis, "Diagnosis of osteoporosis and assessment of fracture risk," *The Lancet*, vol. 359, no. 9321, pp. 1929–1936, 2002.
- [73] J. A. Kanis, F. Borgstrom, C. De Laet, H. Johansson, O. Johnell, B. Jonsson, A. Oden, N. Zethraeus, B. Pflieger, and N. Khaltayev, "Assessment of fracture risk," *Osteoporosis International*, vol. 16, no. 6, pp. 581–589, 2005.

- [74] M. Van der Meulen, K. Jepsen, and B. Miki, "Understanding bone strength: size isn't everything," *Bone*, vol. 29, no. 2, pp. 101–104, 2001.
- [75] E. Donnelly, "Methods for assessing bone quality: A review," *Clinical Orthopaedics and Related Research*, vol. 469, no. 8, pp. 2128–2138, 2011. [Online]. Available: <http://dx.doi.org/10.1007/s11999-010-1702-0>
- [76] S. Judex, S. Boyd, Y.-X. Qin, L. Miller, R. Mller, and C. Rubin, "Combining high-resolution micro-computed tomography with material composition to define the quality of bone tissue," *Current osteoporosis reports*, vol. 1, no. 1, pp. 11–19, 2003.
- [77] E. Seeman and P. D. Delmas, "Bone quality: the material and structural basis of bone strength and fragility," *New England Journal of Medicine*, vol. 354, no. 21, pp. 2250–2261, 2006.
- [78] M. E. Launey, M. J. Buehler, and R. O. Ritchie, "On the mechanistic origins of toughness in bone," *Annual Review of Materials Research*, vol. 40, no. 1, pp. 25–53, 2010. [Online]. Available: <http://www.annualreviews.org/doi/abs/10.1146/annurev-matsci-070909-104427>
- [79] M. Saito and K. Marumo, "Collagen cross-links as a determinant of bone quality: a possible explanation for bone fragility in aging, osteoporosis, and diabetes mellitus," *Osteoporosis international*, vol. 21, no. 2, pp. 195–214, 2010.
- [80] D. R. Taaffe, C. Snow-Harter, D. A. Connolly, T. L. Robinson, M. D. Brown, and R. Marcus, "Differential effects of swimming versus weight-bearing activity on bone mineral status of eumenorrhic athletes," *J Bone Miner Res*, vol. 10, no. 4, pp. 586–93, 1995. [Online]. Available: <http://www.ncbi.nlm.nih.gov/pubmed/7610929>
- [81] J. Morel, B. Combe, J. Francisco, and J. Bernard, "Bone mineral density of 704 amateur sportsmen involved in different physical activities," *Osteoporos Int*, vol. 12, no. 2, pp. 152–7, 2001. [Online]. Available: <http://www.ncbi.nlm.nih.gov/pubmed/11303716>
- [82] S. Bourrin, F. Ghaemmaghami, L. Vico, D. Chappard, C. Gharib, and C. Alexandre, "Effect of a five-week swimming program on rat bone: A histomorphometric study," *Calcified Tissue International*, vol. 51, no. 2, pp. 137–142, 1992. [Online]. Available: <http://dx.doi.org/10.1007/BF00298502>
- [83] T.-H. Huang, S. S. Hsieh, S.-H. Liu, F.-L. Chang, S.-C. Lin, and R.-S. Yang, "Swimming training increases the post-yield energy of bone in young male rats," *Calcified tissue international*, vol. 86, no. 2, pp. 142–153, 2010.
- [84] H. Isaksson, V. Tolvanen, M. A. Finnil, J. Iivarinen, J. Tuukkanen, K. Seppnen, J. P. Arokoski, P. A. Brama, J. S. Jurvelin, and H. J. Helminen, "Physical exercise improves properties of bone and its collagen network in growing and maturing mice," *Calcified tissue international*, vol. 85, no. 3, pp. 247–256, 2009.
- [85] J. M. Wallace, M. S. Ron, and D. H. Kohn, "Short-term exercise in mice increases tibial post-yield mechanical properties while two weeks of latency following exercise increases tissue-level strength," *Calcified tissue international*, vol. 84, no. 4, pp. 297–304, 2009.

- [86] S. J. Warden, R. K. Fuchs, A. B. Castillo, I. R. Nelson, and C. H. Turner, "Exercise when young provides lifelong benefits to bone structure and strength," *Journal of Bone and Mineral Research*, vol. 22, no. 2, pp. 251–259, 2007. [Online]. Available: <http://dx.doi.org/10.1359/jbmr.061107>
- [87] D. H. Kohn, N. D. Sahar, J. M. Wallace, K. Golcuk, and M. D. Morris, "Exercise alters mineral and matrix composition in the absence of adding new bone," *Cells Tissues Organs*, vol. 189, no. 1-4, pp. 33–7, 2009. [Online]. Available: <http://www.ncbi.nlm.nih.gov/pubmed/18703871>
- [88] L. Mosekilde, C. Danielsen, C. Sgaard, and E. Thorling, "The effect of long-term exercise on vertebral and femoral bone mass, dimensions, and strength assessed in a rat model," *Bone*, vol. 15, no. 3, pp. 293–301, 1994.

2. IN VIVO TIBIAL LOADING OF OSTEOLATHRYTIC MICE INDUCED BY A LONG-TERM LOW-DOSE TREATMENT OF BAPN

2.1 Introduction

The goal of this initial study was to observe the effects of tibial loading in a disease state that primarily affects bone quality. Osteolathyrism, induced by treatment with β -aminopropionitrile (BAPN), is a disease characterized by a reduction in enzymatic cross-linking [1,2], resulting in decreased strength of the bone tissue [3]. BAPN irreversibly binds to lysyl oxidase, an enzyme involved in the formation and maturation of enzymatic cross-links in collagen-based tissues, including bone [4,5]. As such, BAPN only affects newly formed cross-links, making the presence of the disease state dependent on the amount of cross-linking occurring. Due to its pathway of action, treatment with BAPN directly affects the collagen portion of bone, resulting in a quality-based bone disease.

In contrast, tibial loading (and mechanical stimulation as a whole) has been shown to improve bone mechanical properties, including stiffness and strength. In addition, studies of other loading regimes (such as exercise and ulnar loading) have shown improvements in collagen-based parameters such as fatigue-loading [6,7] and post-yield mechanical properties [8,9] suggesting that tibial loading may result in similar effects. Considering the decrease in collagen quality that occurs with BAPN treatment, and the increase in collagen quality that can occur with mechanical stimulation, the working hypothesis of this study was that tibial loading would be able to improve bone mechanical properties in healthy and osteolathrytic mice.

Previous work in our lab indicated that 2 weeks of BAPN treatment was insufficient to induce a disease state in bone [10]. Thus, a long-term (7 week) BAPN

treatment study was performed. For the study, BAPN and control (CON) mice were injected subcutaneously with either BAPN or phosphate-buffered solution (PBS) daily, respectively, beginning at 4 weeks of age. At 8 weeks of age, $n = 5$ BAPN and CON mice were sacrificed as a baseline to perform a load/strain calibration. The remaining mice continued with daily injections, and their right tibiae were loaded for 3 days, followed by 2 days of rest, repeated 4 times over the course of 3 weeks. At 11 weeks of age, the remaining mice were euthanized. This setup allowed observation of the disease progression (after 0 weeks, 4 weeks, and 7 weeks of treatment). In addition, the use of tibial loading enabled the contralateral limb of each mouse to act as its own internal control, and allowed us to explore the effect of load on the diseased and non-diseased mice.

While the study was designed to address the above-mentioned questions, the results indicated a lack of a functional disease state, lending this study more of an observation regarding the effect of mechanical stimulation rather than an understanding of how mechanical stimulation affects disease. Due to the lack of effects of BAPN, the next chapter explores the use of a higher dose of BAPN treatment as a means of inducing a disease.

2.2 Methods

2.2.1 Animals

All animal procedures were performed with prior approval from the Indiana University School of Science Institutional Animal Care and Use Committee (IACUC). Fifty-one C57Bl6 mice (Harlan Laboratories) were obtained at 3 weeks of age and allowed to acclimate for one week prior to the start of the study. At four weeks of age, five weight-matched mice were euthanized and their tibiae were harvested as a pre-injection baseline. The remaining 46 mice were divided into two weight matched groups: β -aminopropionitile (BAPN; $n = 23$) and control (CON; $n = 23$). The BAPN group was subcutaneously injected each day with 164 mg/kg of BAPN

(300 mg/kg of BAPN fumarate) dissolved in 200 μ L of sterile PBS, while the CON group was injected with same volume of sterile PBS. Throughout the study, mice were weighed every other day to assess health and maintain a constant drug dosage.

2.2.2 Strain Calibration

After four weeks of injections, five weight-matched mice from each group were used for a strain gage calibration, as previously described [11]. Briefly, mice were anesthetized with isoflurane. An incision was made through the skin of the right tibia and the underlying bone was exposed. A strain gage was then attached using cyanoacrylate to the anteromedial portion of the bone, proximal to the tibia-fibula junction. After attachment, the strain gage was coated with polyurethane. The right tibia of each mouse was then cyclically loaded in a mechanical tester from 1 to 10 N in 1 N increments, and the resulting strain was recorded. After the calibration, mice were immediately euthanized and their tibiae harvested as a pre-loading baseline. Due to complications with the placing of the strain gage, two mice per group were removed from analysis.

2.2.3 *In vivo* Loading

Based on the results of the strain calibration, the right tibiae of the remaining mice ($n = 18$ BAPN and $n = 18$ CON) were loaded daily for three days followed by a two day rest, and repeated four times for a total of 12 bouts of loading over a three week period. The contralateral limb acted as an internal, non-loaded control. Each loading bout consisted of 220 cycles, split into 4 loading cycles at 2 Hz followed by 3 seconds of rest, and repeated 55 times. For the first three days, the CON and BAPN mice were loaded to 11.1 and 9.8 N, respectively (engendering 2100 $\mu\varepsilon$). Also for the first three days, the rest period was held at 0.3 N. However, after three days of loading, it was noted that the mice were limping and it was determined that holding the load at 0.3 N caused the mechanical testing actuator to jump slightly upon

reloading to maximum load level, possibly causing injury. For that reason, the load during the rest period was switched to the high load level, as previously performed in the lab. In addition, the maximum compressive load was dropped to 10.0 and 8.9 N, respectively (engendering 1900 $\mu\epsilon$), for the remainder of the loading bouts. This response of the mice to loading will be explored later in Chapter 4. During the three weeks of loading, mice were injected daily with either PBS or BAPN.

At 11 weeks of age, the mice were euthanized by CO₂ asphyxiation. The right and left tibiae were harvested, wrapped in saline-soaked gauze, and stored at -20 °C for analysis.

2.2.4 Micro Computed Tomography (μ CT)

All tibiae were thawed to room temperature and scanned by μ CT. During scanning, each tibia was wrapped in parafilm to maintain hydration and then scanned at a 9.8 μm voxel resolution. Calibration was performed using two hydroxyapatite phantoms (0.25 and 0.75 g/cm³) in order to calculate mineral density from the grayscale values. Images were reconstructed using NRecon and analysis was performed on cortical and trabecular regions of interest (ROI). Of the tibiae imaged, 10 right and left BAPN and CON tibiae were used for μ CT analysis and mechanical testing, while the remaining 8 right and left BAPN and CON tibiae were used for fracture toughness testing.

For cortical analysis, an ROI was selected as seven transverse slices centered at 50% of the bone length. Tissue mineral density (TMD) was calculated using vendor-supplied software (CTAn). A binary threshold was then applied to the slices and geometric properties were calculated using a custom MATLAB code. Output parameters include total cross sectional area (tCSA), medullary area (Med.Ar), cortical area (Ct.Ar), cortical thickness (Ct.Th), periosteal bone surface (pBS), endocortical bone surface (eBS), the moment of inertia about the anterior-posterior axis (Iap), the moment of inertia about the medial-lateral axis (Iml), and tissue mineral density

(TMD). In addition, average cortical profiles for each group were created to aid with visualization. To better enable an assessment of the effects of age, the cortical profiles at 4 and 8 weeks of age were also created and compared to those at 11 weeks; however, no statistical analyses were performed at 4 and 8 weeks of age.

Trabecular analysis was performed on an ROI defined as 6% of the total bone length, beginning at the end of the proximal growth plate and extending distally. Within that region, the trabecular section was automatically segmented from the cortical outer shell using a custom MATLAB script. Geometric properties (bone volume fraction (BV/TV), trabecular thickness (Tb.Th), separation (Tb.Sp), and number (Tb.N), and tissue mineral density (TMD)) were calculated using vendor-supplied software (CTAn).

2.2.5 Mechanical Testing

Following μ CT, tibiae were tested to failure in four-point bending (9 mm outer span; 3 mm inner span). A displacement rate of 0.025 mm/sec was used. The tibiae were oriented in the medial-lateral direction with the medial side in tension. After failure, the distance from the proximal end of the bone to the site of fracture was recorded. Seven slices at the site of fracture were pulled from the μ CT data and used to normalize load and displacement into stress and strain, respectively. Structural-level and tissue-level mechanical properties were then obtained from the load-displacement and stress-strain curves.

2.2.6 Fracture Toughness Testing

Fracture toughness testing was performed as previously described [12,13]. Briefly, tibiae were hand-notched with a scalpel blade in the anterior-medial region of the mid-diaphysis, proximal to the tibia-fibula junction such that the notch entered the medullary cavity but did not proceed more than halfway through the bone. During notching, the scalpel blade was lubricated with a 1 μ m diamond suspension. After

notching, bones were tested to failure in three-point bending at 0.001 mm/sec with the notched side in tension and the notch located directly under the applied load. After the test, the distance to the fracture site was measured using calipers, which was then used in conjunction with μ CT to determine geometric properties at the location of fracture. Bones were then dehydrated with graded ethanol (70–100%), and the fracture surface was imaged using scanning electron microscopy (SEM). Images obtained were used to determine the angles of stable and unstable crack growth. Force and displacement data, geometric properties, and the crack growth angles were used in a custom MATLAB script to determine fracture stress intensity (K) values at yield force (crack initiation), at maximum force, and at failure force (crack instability).

2.2.7 Statistics

The data were checked for assumptions of normality and homogeneity of variance, and violations were corrected using transformations. A repeated-measures ANOVA was performed to assess the main effects of disease (between-subject effect), loading (within-subject effect) and their interaction (significance at $p < 0.05$). If the interaction term was significant, main effects were determined using a t-test (effect of disease) or a paired t-test (effect of loading), and a Bonferroni correction was applied ($p < 0.0125$). In the case that normality could not be corrected, a pairwise Mann-Whitney U Test was performed and p-value corrected for multiple comparisons ($p < 0.0125$).

2.3 Results

2.3.1 Animal Weight

Animal weights from the BAPN and CON mice were monitored every other day as a means of checking animal health and ensuring proper dosage of the BAPN drug.

Results indicated no difference between the BAPN and CON groups throughout the study. At harvest, mice weights were 20.46 ± 0.96 g for the CON mice and 20.78 ± 1.45 g for the BAPN mice.

2.3.2 Strain Calibration

The strain calibration was performed on $n = 3$ BAPN and CON mice at 8 weeks of age. The results suggested that the CON mice had slightly stiffer bones, as shown in Figure 2.1; however, the difference was not significant.

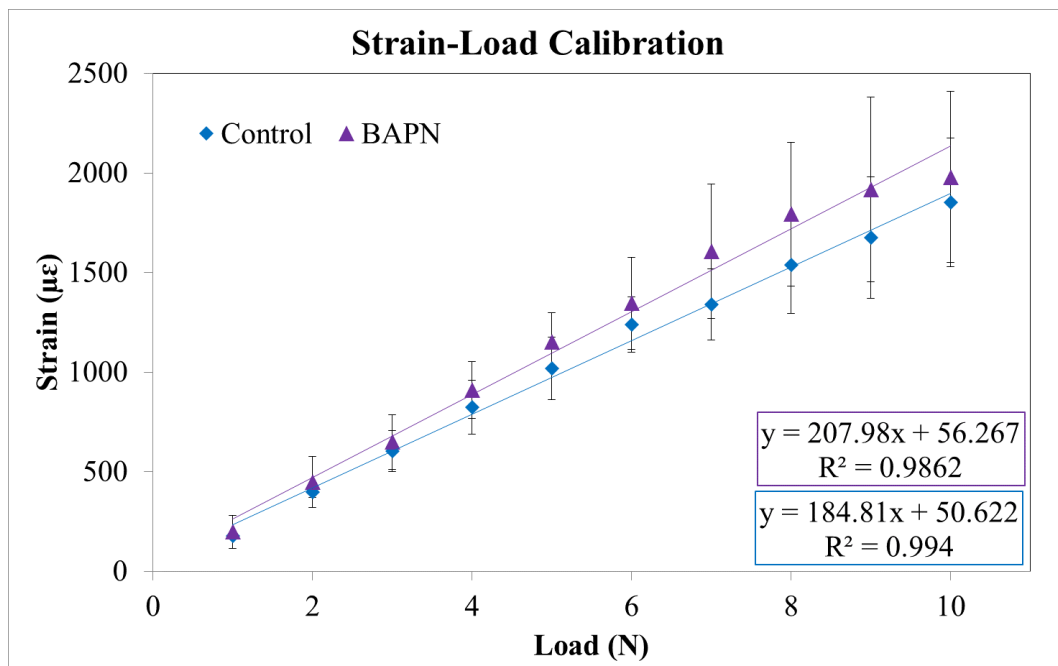


Fig. 2.1. Strain calibration of BAPN and CON mice at 8 weeks of age indicate that CON mice had slightly stiffer bones (not significant). Loading the CON and BAPN mice to 11.1 N and 9.8 N, respectively, engendered $2100 \mu\epsilon$ in both groups.

Based on the results of the strain calibration, CON and BAPN mice were loaded with a dynamic compressive load of 11.1 and 9.8 N, respectively, engendering $2100 \mu\epsilon$ in both groups. Due to observed limping in the animals, after three bouts of loading,

the dynamic load was reduced to 10.0 N for CON and 8.9 N for BAPN, engendering 1900 $\mu\epsilon$ in both groups.

2.3.3 Tibial Morphology

Morphology of the tibia was assessed by μ CT using $n = 10$ BAPN and CON mice. Both cortical and cancellous analyses were performed.

For the cortical section, analysis was performed on the 4 week pre-injection baseline ($n = 5$), 8 week baseline ($n = 5$ BAPN and CON), and 11 week loaded and non-loaded ($n = 10$ BAPN and CON) mice. Slices were taken from the midshaft (50% of the bone length). A clear effect of growth was observed in both groups over the course of the 7 week treatment, especially within the first 4 weeks (Figure 2.2).

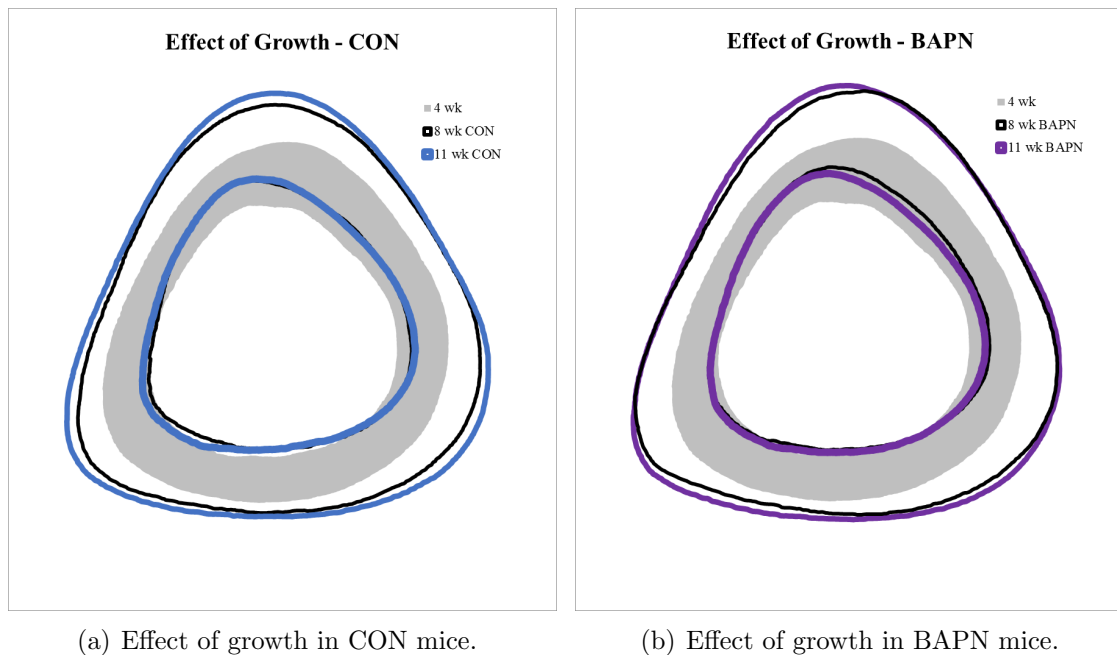


Fig. 2.2. During the 7-week study, significant growth occurred in (a) CON and (b) BAPN mice, especially in the first 4 weeks.

Since BAPN only impacts the formation of cross-links and has no impact on pre-existing cross-links, the significant amount of growth during the treatment period

(from 4 to 11 weeks of age) would suggest that there was ample time to reduce cross-link formation and induce an osteolathrytic disease state.

Interestingly, however, there were only mild effects of BAPN on morphology. A comparison of BAPN and CON at 8 weeks and 11 weeks of age is shown in Figure 2.3.

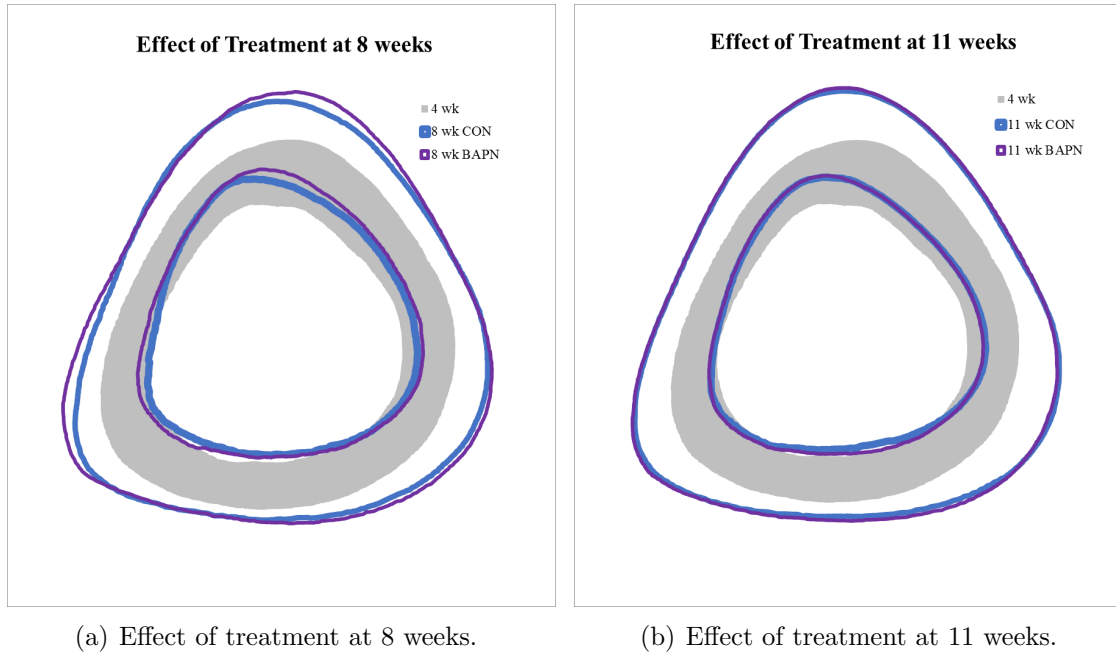


Fig. 2.3. Cortical cross-section of the BAPN mice at (a) 8 weeks and (b) 11 weeks of age indicate that although there was slightly altered morphology in the BAPN mice at 8 weeks of age, those differences vanished at 11 weeks.

Although Figure 2.3(a) suggests a difference in cortical morphology at 8 weeks of age, the results were not significant due to the small sample size. At 11 weeks of age, any potential differences seen at 8 weeks of age vanished, resulting in an almost identical average cross section (Figure 2.3(b)). Statistics indicated that there were a few modest significant effects of BAPN in the loaded limbs (decreased periosteal bone surface and moment of inertia about the medial-lateral axis). However, there were no major changes.

Although the effect of BAPN was minimal, the response to load was robust, shown in Figure 2.4.

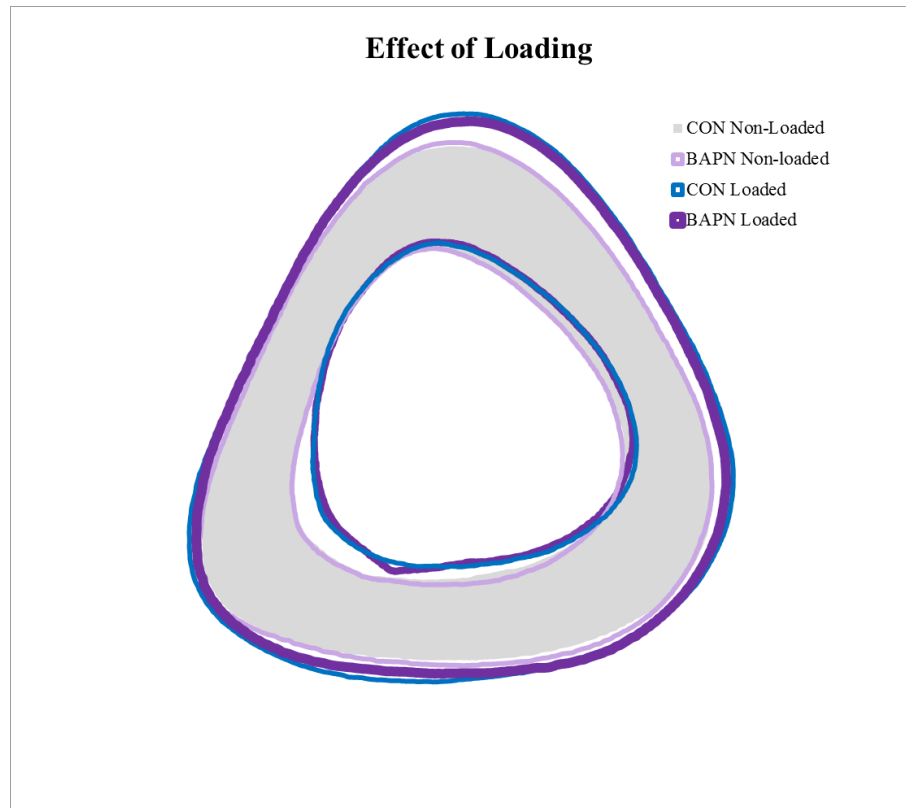


Fig. 2.4. Cortical cross-sections in non-loaded and loaded limbs show a robust response of bone to load. Effects involve both periosteal expansion and cortical contraction.

Loading resulted in periosteal expansion and endocortical contraction in both the CON and BAPN mice. These results are summarized in Table 2.1.

Similar results were observed when analyzing the cancellous architecture. Namely, the effects of BAPN were minimal, while the effects of load were robust. Properties of the cancellous bone are displayed in Table 2.2. Note that one CON mouse was removed from analysis as it was a statistical outlier in many of the properties analyzed.

As stated previously, the effects of BAPN were minimal. Tissue mineral density was significantly decreased with BAPN, but only in the loaded limbs. There were no other significant differences noted with disease. In contrast, loading resulted in robust improvements in cancellous architecture, as can be observed by the significantly

Table 2.1.
Cortical morphology assessed by μ CT

Bone Property	CON		BAPN		Two-way ANOVA		
	Non-Loaded	Loaded	Non-Loaded	Loaded	Disease	Load	Interaction
tCSA (mm ²)	0.943 ± 0.059	1.085 ± 0.033*	0.957 ± 0.057	1.050 ± 0.033*	— ^c	— ^c	0.03
Med.Ar (mm ²)	0.399 ± 0.027	0.392 ± 0.026	0.407 ± 0.024	0.386 ± 0.042	NS	NS	NS
Ct.Ar (mm ²)	0.543 ± 0.040	0.693 ± 0.031	0.549 ± 0.036	0.664 ± 0.023	NS	<.0001	NS
Ct.Th (mm)	0.190 ± 0.010	0.234 ± 0.012	0.191 ± 0.007	0.228 ± 0.014	NS	<.0001	NS
pBS (mm)	4.169 ± 0.132	4.462 ± 0.070*	4.192 ± 0.149	4.367 ± 0.072*#	— ^c	— ^c	0.01
eBS (mm)	2.797 ± 0.107	2.739 ± 0.091	2.814 ± 0.104	2.753 ± 0.153	NS	0.04	NS
Iap (mm ⁴)	0.055 ± 0.007	0.073 ± 0.005	0.056 ± 0.007	0.069 ± 0.004	NS	<.0001	NS
Iml (mm ⁴)	0.066 ± 0.010	0.096 ± 0.006*	0.068 ± 0.009	0.088 ± 0.004*#	— ^c	— ^c	0.03
TMD (g/cm ³)	1.199 ± 0.013	1.202 ± 0.019	1.203 ± 0.013	1.202 ± 0.025	NS	NS	NS

^a Data are mean ± SD

^b tCSA = total cross sectional area; Med.Ar = medullary area; Ct.Ar = cortical area; Ct.Th = cortical thickness;

pBS = periosteal bone surface; eBS = endocortical bone surface; Iap = moment of inertia about the anterior-posterior axis; Iml = moment of inertia about the medial-lateral axis; TMD = tissue mineral density

^c Disease and load main effects were ignored in the presence of a significant Disease*Load interaction

* p < 0.0125 vs non-loaded limb within same disease group (paired t-test)

p < 0.0125 vs CON within same load group (unpaired t-test)

Table 2.2.
Cancellous architecture assessed by μ CT

Bone Property	CON		BAPN		Two-way ANOVA		
	Non-Loaded	Loaded	Non-Loaded	Loaded	Disease	Load	Interaction
BV/TV (%)	8.47 \pm 1.39	8.95 \pm 1.31	9.23 \pm 0.67	8.70 \pm 0.51	NS	NS	NS
Tb.Th (mm)	0.054 \pm 0.002	0.073 \pm 0.005*	0.055 \pm 0.002	0.070 \pm 0.003*	— ^c	— ^c	0.04
Tb.Sp (mm)	0.257 \pm 0.025	0.285 \pm 0.0279	0.241 \pm 0.010	0.273 \pm 0.012	NS	<.0001	NS
Tb.N (1/mm)	1.56 \pm 0.29	1.23 \pm 0.23	1.68 \pm 0.081	1.25 \pm 0.07	NS	<.0001	NS
TMD (g/cm ³)	0.718 \pm 0.007	0.798 \pm 0.018*	0.718 \pm 0.011	0.775 \pm 0.012*#	— ^c	— ^c	0.0025

^a Data are mean \pm SD

^b BV/TV = bone volume fraction; Tb.Th = trabecular thickness; Tb.Sp = trabecular spacing; Tb.N = trabecular number; TMD = tissue mineral density

^c Disease and load main effects were ignored in the presence of a significant Disease*Load interaction

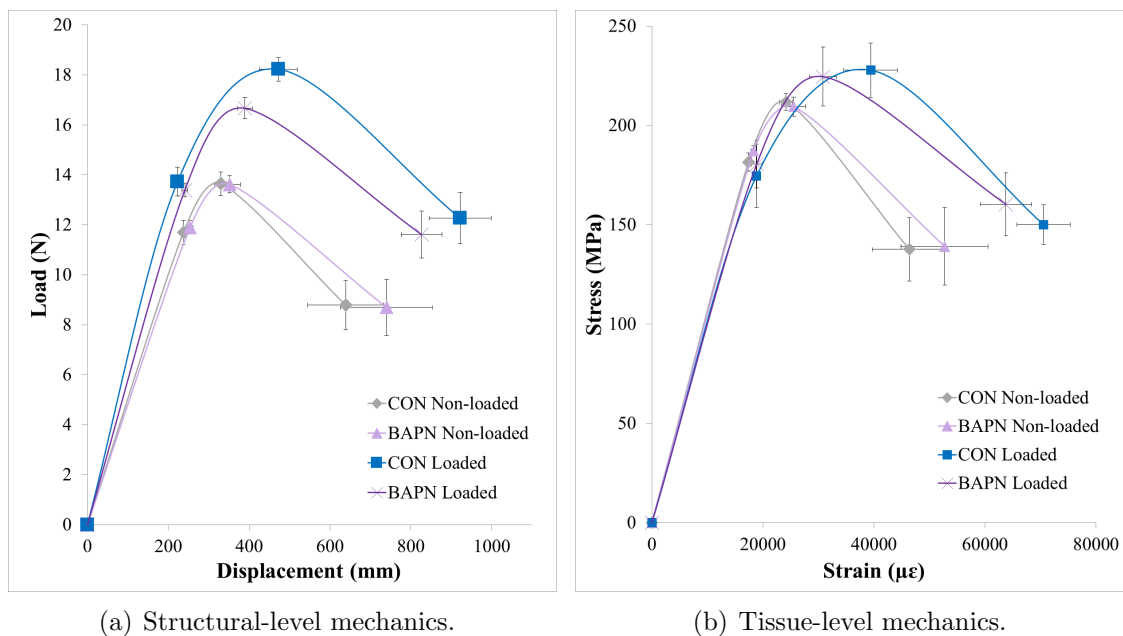
* $p < 0.0125$ vs non-loaded limb within same disease group (paired t-test)

$p < 0.0125$ vs CON within same load group (unpaired t-test)

improved trabecular thickness and tissue mineral density. Interestingly, loading also negatively impacted trabecular separation and trabecular number, resulting in fewer, thicker trabeculae that had greater separation between them.

2.3.4 Tibial Mechanics

The tibiae used for CT analysis were then tested in four-point bending to assess mechanical integrity. Representative graphs of the force-displacement and stress-strain curves for each group are shown in 2.5. Statistics were not performed on the representative graphs, but instead serve to illustrate differences.



(a) Structural-level mechanics.

(b) Tissue-level mechanics.

Fig. 2.5. Representative Force-Displacement and Stress-Strain curves show a robust response of load in terms of structure-level properties. When normalized by cross-sectional area, the effect of load is less pronounced. Treatment with BAPN had no effect on the mechanics.

From the load-displacement graph 2.5(a), it is clear that the loaded limbs were stiffer and able to maintain higher forces before breaking. The stress-strain graph 2.5(b) suggests a similar trend; however, the difference is not as pronounced due to

the large increase in the loaded bones cross-sectional area as noted in the previous section. In contrast to the effects of load, there was no clear effect of BAPN treatment on bone mechanics. These results are summarized in Table 2.3 and 2.4.

2.3.5 Fracture Toughness

Fracture toughness was performed on the right and left tibiae of 8 CON and BAPN mice. Results showed no significant effects of either load or BAPN treatment. Results are tabulated in Table 2.5.

2.4 Discussion

Altogether, the results of this study showed minimal effects of BAPN and a robust effect of tibial loading on bone mass and mechanics (larger effect in structural-level, rather than tissue-level, mechanics). Due to the lack of effects of disease, this study was unable to answer the initial research question as to the ability of tibial loading to improve bone quality in a disease state; however, the study did produce interesting results with respect to the effect of tibial loading itself.

2.4.1 Little Effect of BAPN Treatment

This study was initially designed as a means of understanding if mechanical stimulation could improve bone quality in a mouse model of osteolathyris. However, based on the results, we were unable to induce a disease state with BAPN. While we did not measure enzymatic cross-linking, the lack of effects in both morphology and mechanics would suggest the lack of a functional disease. A full discussion of this topic will be included in the next chapter. For now, the limited effects observed after 7 weeks of a low-dose treatment of BAPN resulted in the decision to increase the dose and repeat the study. That study and a discussion of both studies are included

Table 2.3.
Structural-level bone mechanical properties

Bone Property	CON		BAPN		Two-way ANOVA		
	Non-Loaded	Loaded	Non-Loaded	Loaded	Disease	Load	Interaction
Yield Force (N)	11.7 ± 1.5	13.7 ± 1.8	11.9 ± 0.9	13.4 ± 0.9	NS	<.0001	NS
Ultimate Force (N)	13.6 ± 1.5	18.2 ± 1.5*	13.6 ± 1.1	16.7 ± 1.4*	— ^b	— ^b	0.044
Disp to Yield (μm)	238 ± 17	232 ± 34	254 ± 23	241 ± 23	NS	NS	NS
Postyield Disp (μm)	404 ± 286	690 ± 243	487 ± 355	586 ± 168	NS	NS	NS
Total Disp (μm)	639 ± 296	922 ± 242	740 ± 359	827 ± 159	NS	NS	NS
Stiffness (N/mm)	57.4 ± 11.7	67.6 ± 9.0	54.1 ± 8.4	63.6 ± 9.3	NS	0.0001	NS
Work to Yield (mJ)	1.54 ± 0.14	1.78 ± 0.43	1.67 ± 0.11	1.78 ± 0.16	Mann-Whitney U Test		
Postyield Work (mJ)	4.09 ± 2.55	9.51 ± 2.40	4.39 ± 2.72	8.01 ± 2.01	NS	0.0002	NS
Total Work (mJ)	5.65 ± 2.54	11.29 ± 2.46	6.05 ± 2.70	9.79 ± 1.94	NS	0.0001	NS

^a Data are mean ± SD

^b Disease and load main effects were ignored in the presence of a significant Disease*Load interaction

* p < 0.0125 vs non-loaded limb within same disease group (paired t-test)

p < 0.0125 vs CON within same load group (unpaired t-test)

Table 2.4.
Tissue-level bone mechanical properties

Bone Property	CON		BAPN		Two-way ANOVA	
	Non-Loaded	Loaded	Non-Loaded	Loaded	Disease	Load Interaction
Yield Stress (MPa)	182 ± 14	175 ± 50	183 ± 15	181 ± 38	Mann-Whitney U Test	Mann-Whitney U Test
Ultimate Stress (MPa)	212 ± 13	228 ± 44	210 ± 15	225 ± 47	Mann-Whitney U Test	Mann-Whitney U Test
Strain to Yield (mε)	17.4 ± 1.3	18.9 ± 2.1	18.4 ± 1.6	18.9 ± 3.0	NS	NS
Total Strain (mε)	46.4 ± 21.2	75.7 ± 21.6	52.8 ± 24.8	63.8 ± 14.5	NS	NS
Modulus (GPa)	12.1 ± 1.7	10.6 ± 3.3	11.5 ± 1.6	11.4 ± 3.9	Mann-Whitney U Test	Mann-Whitney U Test
Resilience (MPa)	1.76 ± 0.13	1.82 ± 0.58	1.86 ± 0.16	1.84 ± 0.26	Mann-Whitney U Test	Mann-Whitney U Test
Toughness(MPa)	6.80 ± 3.17	11.4 ± 2.7	7.34 ± 3.31	10.8 ± 2.7	NS	NS

^a Data are mean ± SD

^b Disease and load main effects were ignored in the presence of a significant Disease*Load interaction

* p < 0.0125 vs non-loaded limb within same disease group (paired t-test)

p < 0.0125 vs CON within same load group (unpaired t-test)

Table 2.5.
Fracture stress intensity values assessed by fracture toughness

Bone Property	CON		BAPN		Two-way ANOVA		
	Non-Loaded	Loaded	Non-Loaded	Loaded	Disease	Load	Interaction
K, init (MPa \sqrt{m})	4.72 \pm 0.66	4.54 \pm 0.36	4.64 \pm 0.41	5.12 \pm 0.58	NS	NS	NS
K, max load (MPa \sqrt{m})	6.02 \pm 0.71	5.98 \pm 0.28	6.11 \pm 0.52	6.59 \pm 0.69	NS	NS	NS
K, inst (MPa \sqrt{m})	7.09 \pm 0.71	7.06 \pm 0.49	6.67 \pm 1.11	8.25 \pm 1.63	NS	NS	NS

^a Data are mean \pm SD

^b K_{,init} = initial fracture toughness resistance; K_{,max load} = fracture toughness resistance at maximum load;

K_{,inst} = fracture toughness resistance at failure

^c There were no statistically significant results

in the next chapter. The remainder of this discussion will be focused on the effect of tibial loading.

2.4.2 Robust Bone Formation Response Due to Loading

While there was little effect of disease, the response to load was robust. In terms of the cancellous bone, loading resulted in thicker trabeculae and higher tissue mineral density. Interestingly, loading also resulted in increased separation and decreased number of trabeculae, which are considered negative effects. One possible explanation is that the damaged accrued in the cancellous region caused reabsorption to occur, resulting in decreased number and increased spacing. At the same time, the loading itself may have caused increased bone mass on the trabeculae that remained, resulting in a seeming dichotomy of results.

Analysis of the cortical bone showed loading-induced increases in cross-sectional area, cortical area, and cortical thickness, resulting in higher moments of inertia. These morphological increases translated to mechanical benefits, with increased strength and stiffness, similar to what was shown previously [11]. After normalizing for the size and shape of the bone, some mechanical effects were still observed but they were more modest, indicating that the primary response to this method of loading was to increase bone mass.

2.4.3 Minimal Effects of Loading on Bone Quality

While the response to load was robust in terms of cancellous and cortical architecture, as well as in terms of bone mechanical behavior as measured by monotonic four-point bending tests, these results were not translated into improved bone quality, as assessed by fracture toughness. In fact, it is interesting to note that the fracture toughness testing showed little difference between loaded and non-loaded tibiae in CON mice. In BAPN mice, the test showed some improvement, but was unable to reach significance for any of the three measures of toughness. These results were

unexpected in that there was an assumption that loading which improved quantity would also improve quality, as has been shown in other loading models [6–9]. However, as discussed in the introduction, that is not always the case, and in this study, the two were not linked.

The question then remains as to why. It is possible that the loading method (tibial loading) had some effect on the output. In the previous studies where a quality effect was noted, models of ulnar loading and exercise were used, whereas in this study, tibial loading was employed. However, ulnar and tibial loading are similar techniques (both are external, non-invasive loading regimens) and thus, if ulnar loading were to show improved bone quality, it would be expected that tibial loading would, as well.

An alternate explanation could be that this lack of effect was due to pain (as indicated by the limping that was observed in the mice following loading). As stated in the methods section, after 3 days of loading, it was noticed that the mice were limping, causing us to decrease the load level on the remaining days. At the same time, we switched from holding the rest load level at 0.3 N to holding the rest load at the high load level. For previous studies in our lab [11], the load had been held at the high load level during the rest period. However, when beginning this study, the resting load was switched to the low load level as it was thought that doing so would allow for better recovery of the mice, which was not the case.

The reason for the increased limping may be related to the control system of the loading device. Namely, during the 3 second rest period, the distance between the loading fixtures increased (through creep). Then, when the rest period was finished, the distance between the fixtures rapidly decreased in order to reach the desired peak load level. This rapid compression was thought to be the cause of injury to the animals. For that reason, after the first three day loading period, the hold level was switched back to the high load level and continued in that way for the remainder of the study.

Although the limping was not extreme and the mice continued to gain weight and groom themselves regularly, it is possible that the limping was indicative of an injury response, which ultimately reduced or negated a quality-based effect. The limping may have been a sign of injury, which caused the bone to respond by rapidly increasing mass to the negligence of bone quality. In any case, the robust structural mechanical improvements but modest tissue level changes and lack of change in fracture toughness suggest that although the loading resulted in improved mass, these effects were mostly decoupled from quality-based improvements.

This result, in combination with the results of the next study, led to the study in Chapter 4, wherein we explore the effect of various loading regimes on mouse pain and bone morphology.

2.5 Conclusion

Injection of a low dose of BAPN in mice from 4 to 11 weeks of age resulted in few changes to bone morphology or mechanics. In contrast, tibial loading increased cortical cross-sectional area and led to larger trabeculae, which translated into increased strength. These results did not extend to improved bone quality as assessed by fracture toughness. This lack of an effect may be due to the limping observed in mice; however, such a hypothesis requires further exploration. As a result of this study, two additional studies were performed: the first (discussed in the next chapter) explored a higher dose of BAPN while the second study (discussed in the following chapter) explored the pain response in mice due to various loading regimens.

2.6 Acknowledgments

We would like to acknowledge the Integrated Nanosystems Development Institute for use of their JSM-7800F system, which was awarded through the National Science Foundation MRI-1229514 grant.

2.7 References

- [1] P. Bornstein, “The cross-linking of collagen and elastin and its inhibition in osteolathyrism,” *The American Journal of Medicine*, vol. 49, no. 4, pp. 429–435, 1970. [Online]. Available: <http://www.sciencedirect.com/science/article/pii/S0002934370800365>
- [2] M. Yamauchi and M. Sricholpech, “Lysine post-translational modifications of collagen,” *Essays Biochem*, vol. 52, pp. 113–33, 2012. [Online]. Available: <http://www.ncbi.nlm.nih.gov/pubmed/22708567>
- [3] E. M. B. McNerny, B. Gong, M. D. Morris, and D. H. Kohn, “Bone fracture toughness and strength correlate with collagen cross-link maturity in a dose-controlled lathyrism mouse model,” *Journal of Bone and Mineral Research*, vol. 30, no. 3, pp. 455–464, 2015. [Online]. Available: <http://dx.doi.org/10.1002/jbmr.2356>
- [4] S. R. Pinnell and G. R. Martin, “The cross-linking of collagen and elastin: enzymatic conversion of lysine in peptide linkage to alpha-amino adipic-delta-semialdehyde (allysine) by an extract from bone,” *Proceedings of the National Academy of Sciences*, vol. 61, no. 2, pp. 708–716, 1968.
- [5] R. C. Siegel, S. R. Pinnell, and G. R. Martin, “Cross-linking of collagen and elastin. properties of lysyl oxidase,” *Biochemistry*, vol. 9, no. 23, pp. 4486–4492, 1970. [Online]. Available: <http://dx.doi.org/10.1021/bi00825a004>
- [6] S. J. Warden, R. K. Fuchs, A. B. Castillo, I. R. Nelson, and C. H. Turner, “Exercise when young provides lifelong benefits to bone structure and strength,” *Journal of Bone and Mineral Research*, vol. 22, no. 2, pp. 251–259, 2007. [Online]. Available: <http://dx.doi.org/10.1359/jbmr.061107>
- [7] D. H. Kohn, N. D. Sahar, J. M. Wallace, K. Golcuk, and M. D. Morris, “Exercise alters mineral and matrix composition in the absence of adding new bone,” *Cells Tissues Organs*, vol. 189, no. 1-4, pp. 33–7, 2009. [Online]. Available: <http://www.ncbi.nlm.nih.gov/pubmed/18703871>
- [8] J. M. Wallace, R. M. Rajachar, M. R. Allen, S. A. Bloomfield, P. G. Robey, M. F. Young, and D. H. Kohn, “Exercise-induced changes in the cortical bone of growing mice are bone and gender specific,” *Bone*, vol. 40, no. 4, pp. 1120–1127, 2007. [Online]. Available: <http://www.ncbi.nlm.nih.gov/pmc/articles/PMC2729655/>
- [9] J. M. Wallace, M. S. Ron, and D. H. Kohn, “Short-term exercise in mice increases tibial post-yield mechanical properties while two weeks of latency following exercise increases tissue-level strength,” *Calcified tissue international*, vol. 84, no. 4, pp. 297–304, 2009.
- [10] C. A. Clauser, “In vivo tibial loading of healthy and osteolathrytic mice,” Thesis, 2015.
- [11] A. G. Berman, C. A. Clauser, C. Wunderlin, M. A. Hammond, and J. M. Wallace, “Structural and mechanical improvements to bone are strain dependent with axial compression of the tibia in female c57bl/6 mice,” *PloS one*, vol. 10, no. 6, p. e0130504, 2015.

- [12] M. A. Hammond, A. G. Berman, R. Pacheco-Costa, H. M. Davis, L. I. Plotkin, and J. M. Wallace, “Removing or truncating connexin 43 in murine osteocytes alters cortical geometry, nanoscale morphology, and tissue mechanics in the tibia,” *Bone*, vol. 88, pp. 85–91, 2016.
- [13] R. Ritchie, K. Koester, S. Ionova, W. Yao, N. Lane, and J. Ager, “Measurement of the toughness of bone: a tutorial with special reference to small animal studies,” *Bone*, vol. 43, no. 5, pp. 798–812, 2008.

3. IN VIVO TIBIAL LOADING OF OSTEOLATHRYTIC MICE INDUCED BY A LONG-TERM HIGH-DOSE TREATMENT OF BAPN

3.1 Introduction

Treatment of mice with a low dose of β -aminopropionitrile (BAPN) over a long-term period (7 weeks) was unable to induce a disease phenotype. For that reason, a second BAPN study was performed at more than double the dose (350 mg/kg in the current study versus 164 mg/kg in the previous study). The same study design from Chapter 2 was employed (7 weeks of injections, with the last 3 weeks also including tibial loading). Analysis consisted of computed tomography and mechanical testing. Due to the similarities between studies, the details in the methods section are shortened.

3.2 Methods

3.2.1 Animals

All animal procedures were performed with prior approval from the Indiana University School of Science Institutional Animal Care and Use Committee (IACUC). As before, female C57Bl6 mice (Harlan Laboratories; $n = 45$) were obtained at 3 weeks of age and allowed to acclimate for one week prior to the start of the study. At four weeks of age, five weight-matched mice were euthanized and their tibiae harvested as a pre-injection baseline. The remaining 40 mice were divided into two weight matched groups: β -aminopropionitrile (BAPN; $n = 20$) and control (CON; $n = 20$). The BAPN group was subcutaneously injected each day with 350 mg/kg of BAPN (640 mg/kg of BAPN fumarate) dissolved in 200 μ L sterile phosphate

buffered saline (PBS) solution, while the CON group was injected with same volume of sterile PBS. Throughout the study, mice were weighed every other day to assess health and maintain constant drug dosage.

3.2.2 Strain Calibration

After four weeks of injections, four weight-matched mice from each group were used for a strain gage calibration, as described above. After the calibration, mice were immediately euthanized and their tibiae were harvested as a pre-loading baseline. An additional 6 mice per group were also euthanized at 8 weeks of age and their tibiae harvested. Due to complications with the placing of the strain gage, one mouse from the CON group was removed from analysis.

3.2.3 *In vivo* Loading

Based on the results of the strain calibration, the right tibiae of the remaining mice ($n = 10$ BAPN and $n = 10$ CON) were loaded as described in the Chapter 2. However, due to the limping that was observed in the mice during that study, the rest period was held at the high load level, as was done previously in the lab [1]. Throughout the loading, the CON and BAPN mice were loaded to 9.6 and 9.2 N, respectively (engendering 2100 $\mu\epsilon$ dynamic load). During the three weeks of loading, mice were injected daily with either PBS or BAPN.

At 11 weeks of age, the mice were euthanized by CO₂ asphyxiation. The tibiae were harvested, wrapped in saline-soaked gauze, and stored at -20 °C for analysis.

3.2.4 Micro Computed Tomography (μ CT)

All tibiae were scanned and analyzed by μ CT, as described in Chapter 2. After scanning, the tibiae were stored at -20 °C until mechanical testing. Both cortical and cancellous analyses were performed, as was the case for the previous study.

3.2.5 Mechanical Testing

Following μ CT, the tibiae were tested to failure in four-point bending. As before, the tibiae were oriented in the medial-lateral direction with the medial side in tension. After failure, the distance from the proximal end to the site of fracture was recorded. Seven slices at the site of fracture were pulled from the μ CT data and used to normalize load and displacement into stress and strain, respectively. Structural-level and tissue-level mechanical properties were then obtained from the load-displacement and stress-strain curves.

3.2.6 Statistics

Data was checked for assumptions of normality and homogeneity of variance, and violations were corrected using transformations. A repeated-measures ANOVA was performed to assess the main effects of disease (between-subject effect), loading (within-subject effect) and their interaction (significance at $p < 0.05$). If the interaction term was significant, main effects were determined using a t-test (effect of disease) or a paired t-test (effect of loading), and a Bonferroni correction was applied ($p < 0.0125$). In the case that normality could not be corrected, a pairwise Mann-Whitney U Test was performed and p-value corrected for multiple comparisons ($p < 0.0125$).

3.3 Results

3.3.1 Animal Weight

Animal weights from the BAPN and CON mice were monitored every other day as a means of checking animal health and ensuring proper dosage of the BAPN drug. Results indicated no difference between the BAPN and CON groups throughout the study. At harvest, mice weights were 19.54 ± 1.17 g for the CON mice and 19.40 ± 1.21 g for the BAPN mice.

3.3.2 Strain Calibration

The strain calibration was performed on $n = 4$ BAPN and $n = 3$ CON mice at 8 weeks of age. The results suggested that the CON mice had similar bone stiffness, shown in Figure 3.1.

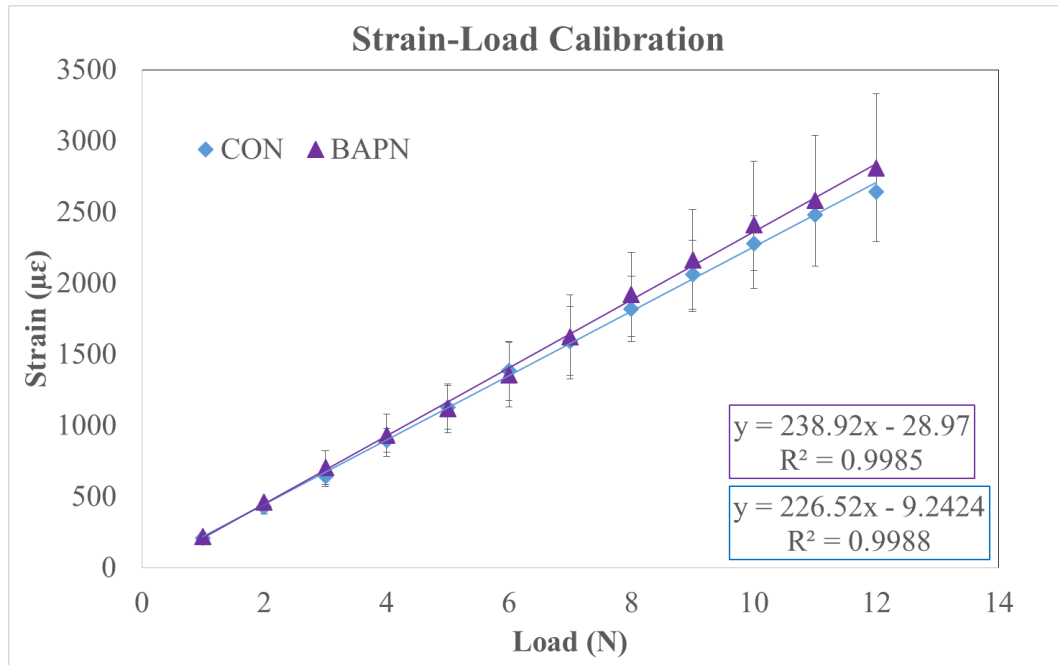


Fig. 3.1. Strain calibration of BAPN and CON mice at 8 weeks of age indicate similar stiffness in CON and BAPN mice. Loading the CON and BAPN mice to 9.6 N and 9.2 N, respectively, engendered 2100 $\mu\epsilon$ in both groups.

Based on the results of the strain calibration, CON and BAPN mice were loaded with a dynamic compressive load of 9.6 and 9.2 N, respectively, engendering 2100 $\mu\epsilon$ in both groups. Despite holding the rest period at the high load level, limping was still observed, though not as severely as was seen in the previous study. For that reason, Chapter 4 explores how to reduce pain during tibial loading.

3.3.3 Tibial Morphology

Morphology of the tibia was assessed by micro-computed tomography using $n = 10$ BAPN and CON mice. Both cortical and cancellous analyses were performed.

For the cortical section, analysis was performed on the 4 week pre-injection baseline ($n = 5$), 8 week baseline ($n = 10$ BAPN and CON), and 11 week loaded and unloaded ($n = 10$ BAPN and CON) mice. Slices were taken from the midshaft (50% of the bone length). As was seen in the previous study, a clear effect of growth was observed in both groups over the course of the 7 week treatment, especially within the first 4 weeks (Figure 3.2).

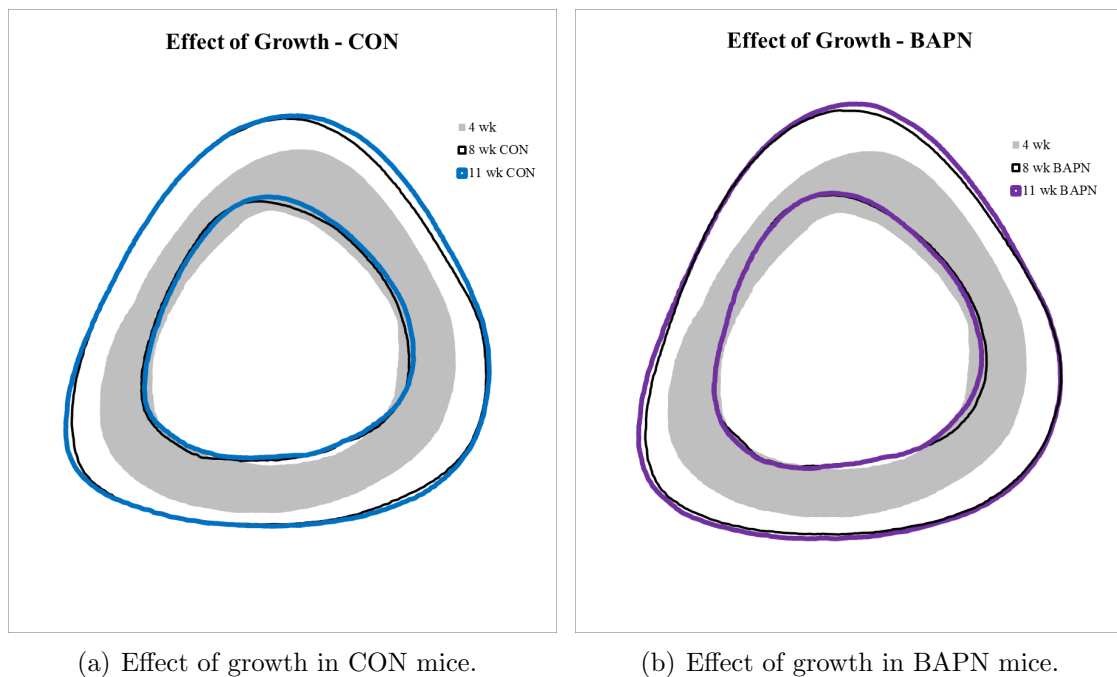


Fig. 3.2. During the 7-week study, significant growth occurred in (a) CON and (b) BAPN mice, especially in the first 4 weeks.

Although there was a large amount of growth over the 7 week study, there were still only mild effects of BAPN on morphology. Figure 3.3 shows a comparison of BAPN and CON at 8 weeks and 11 weeks of age.

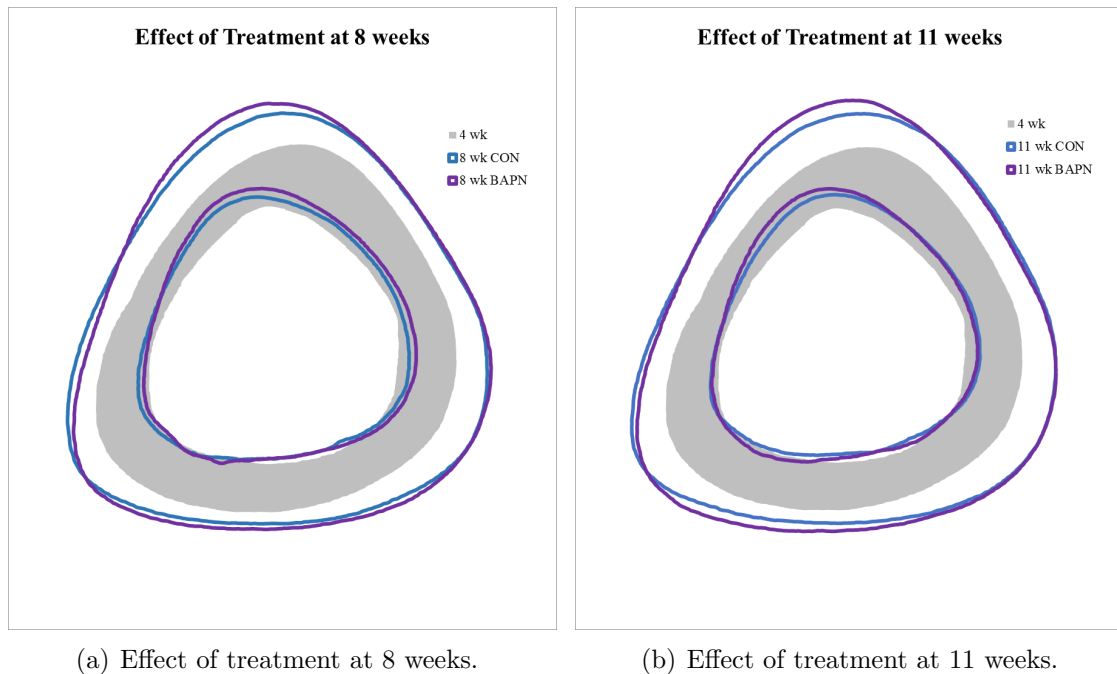


Fig. 3.3. Cortical cross-section of the BAPN mice at (a) 8 weeks and (b) 11 weeks of age indicate slight, but consistent differences in the morphology of BAPN mice at 8 and 11 weeks of age.

As shown in Figure 3.3, there were slight, but consistent, differences between BAPN and CON at 8 and 11 weeks. However, the differences were modest and few properties reached significance (Table 3.1).

Although the effect of BAPN was minimal, the response to load was again robust, shown in Figure 3.4.

Similar to before, loading resulted in periosteal expansion and endocortical contraction in both the CON and BAPN mice. However, unlike before, there were many significant interactions between disease and load. For example, there were effects of load in total cross-sectional area, periosteal bone surface, anterior-posterior width, and moment of inertia about the medial-lateral axis, but these effects were only observed in the CON mice. In contrast, load significantly decreased medullary area in the BAPN mice, but not the CON mice. In addition, in the non-loaded limbs, there was an effect of BAPN on the anterior-posterior width and the moment of inertia

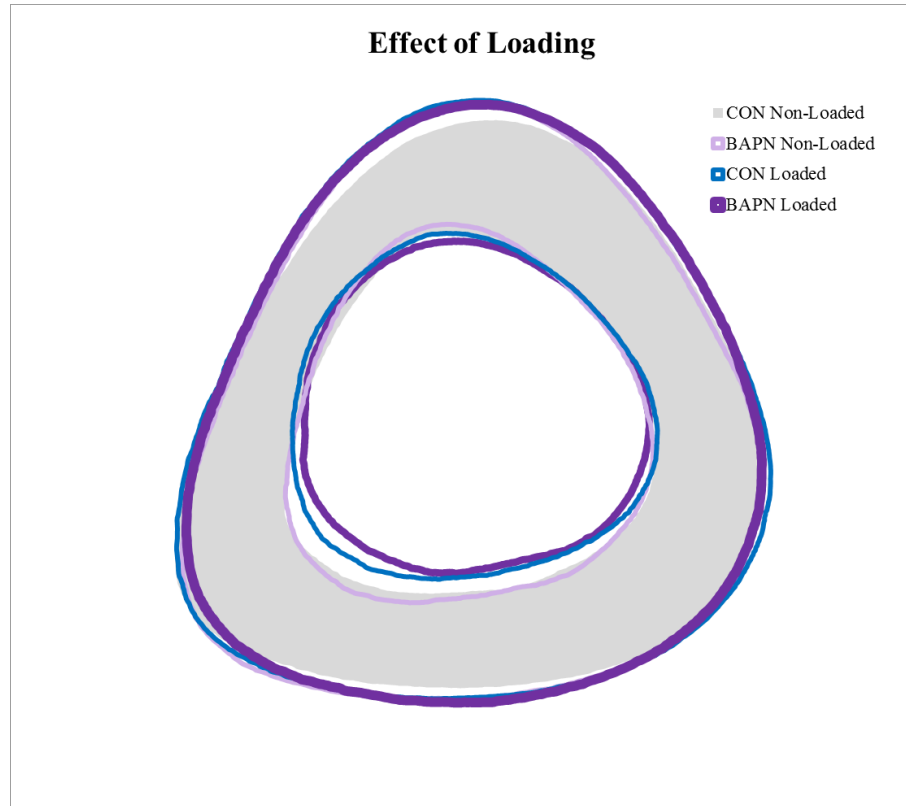


Fig. 3.4. Cortical cross-sections in non-loaded and loaded limbs show a robust response of bone to load. Effects involve both periosteal expansion and cortical contraction.

about the medial-lateral axis, whereas in the loaded limbs, there was a significant effect of BAPN on cortical thickness. These interactions suggest that, although there were only mild effects of BAPN, BAPN altered the tibia's ability to respond to load. These results are summarized in Table 3.1.

In terms of cancellous architecture (Table 3.2), loading resulted in increased thickness but decreased number of trabeculae. Interestingly, the bone volume fraction was decreased with loading in both CON and BAPN; however, the decrease in the BAPN was much larger than in CON (29.0% decrease in BAPN versus 2.5% decrease in CON). In addition, bone mineral density was increased in the CON mice with loading, but was decreased in the BAPN mice with loading. As for the cortical

Table 3.1.
Cortical morphology assessed by μ CT

Bone Property	CON		BAPN		Two-way ANOVA		
	Non-Loaded	Loaded	Non-Loaded	Loaded	Disease	Load	Interaction
tCSA (mm ²)	0.912 ± 0.041	0.968 ± 0.033*	0.937 ± 0.043	0.948 ± 0.045	— ^c	— ^c	0.02
Med.Ar (mm ²)	0.371 ± 0.026	0.356 ± 0.027	0.384 ± 0.026	0.327 ± 0.030*	— ^c	— ^c	0.001
Ct.Ar (mm ²)	0.541 ± 0.024	0.612 ± 0.017	0.553 ± 0.028	0.621 ± 0.022	NS	<.0001	NS
Ct.Th (mm)	0.195 ± 0.007	0.219 ± 0.007*	0.196 ± 0.008	0.228 ± 0.01*#	— ^c	— ^c	0.04
pBS (mm)	4.077 ± 0.108	4.194 ± 0.078*	4.137 ± 0.102	4.135 ± 0.109	— ^c	— ^c	0.02
eBS (mm)	2.682 ± 0.099	2.611 ± 0.106*	2.724 ± 0.101	2.514 ± 0.115*	— ^c	— ^c	0.003
Iap (mm ⁴)	0.057 ± 0.005	0.063 ± 0.004	0.056 ± 0.006	0.060 ± 0.006	NS	0.0002	NS
Iml (mm ⁴)	0.057 ± 0.005	0.069 ± 0.006*	0.064 ± 0.007#	0.069 ± 0.006	— ^c	— ^c	0.04
TMD (g/cm ³)	1.237 ± 0.011	1.239 ± 0.007	1.228 ± 0.012	1.234 ± 0.009	NS	NS	NS

^a Data are mean ± SD

^b tCSA = total cross sectional area; Med.Ar = medullary area; Ct.Ar = cortical area; Ct.Th = cortical thickness;

pBS = periosteal bone surface; eBS = endocortical bone surface; Iap = moment of inertia about the anterior-posterior axis; Iml = moment of inertia about the medial-lateral axis; TMD = tissue mineral density

^c Disease and load main effects were ignored in the presence of a significant Disease*Load interaction

* p < 0.0125 vs non-loaded limb within same disease group (paired t-test)

p < 0.0125 vs CON within same load group (unpaired t-test)

Table 3.2.
Cancellous architecture assessed by μ CT

Bone Property	CON		BAPN		Two-way ANOVA		
	Non-Loaded	Loaded	Non-Loaded	Loaded	Disease	Load	Interaction
BV/TV (%)	8.83 \pm 1.02	8.61 \pm 1.02	8.75 \pm 0.99	6.21 \pm 1.94*#	— ^c	— ^c	0.01
Tb.Th (mm)	0.057 \pm 0.002	0.074 \pm 0.003*	0.056 \pm 0.001	0.071 \pm 0.004*	Mann Whitney U		
Tb.Sp (mm)	0.260 \pm 0.0155	0.283 \pm 0.011	0.255 \pm 0.018	0.318 \pm 0.040	NS	<.0001	NS
Tb.N (1/mm)	1.54 \pm 0.17	1.16 \pm 0.14*	1.57 \pm 0.18	0.88 \pm 0.27*	— ^c	— ^c	0.01
BMD (g/cm ²)	0.113 \pm 0.022	0.118 \pm 0.014	0.117 \pm 0.010	0.072 \pm 0.03*#	— ^c	— ^c	0.001
TMD (g/cm ²)	0.716 \pm 0.0111	0.793 \pm 0.016	0.691 \pm 0.011	0.752 \pm 0.031	<.0001	<.0001	NS

^a Data are mean \pm SD

^b BV/TV = bone volume fraction; Tb.Th = trabecular thickness; Tb.Sp = trabecular spacing; Tb.N = trabecular number; BMD = bone mineral density; TMD = tissue mineral density

^c Disease and load main effects were ignored in the presence of a significant Disease*Load interaction

* p < 0.0125 vs non-loaded limb within same disease group (paired t-test)

p < 0.0125 vs CON within same load group (unpaired t-test)

properties, the results of cancellous analysis suggest that the treatment with BAPN altered the body's ability to respond to mechanical stimulation.

While bone mineral density was indistinguishable between CON and BAPN in the non-loaded limbs (the only effect was in the loaded limbs), tissue mineral density (the density of the bone tissue itself) was significantly decreased with disease and significantly improved with loading. Properties of the cancellous bone are displayed in Table 3.2.

3.3.4 Tibial Mechanics

The tibiae used for CT analysis were then tested to failure in four-point bending to assess mechanical integrity. Representative graphs of the force-displacement and stress-strain curves for each group are shown in Figure 3.5. Statistics were not performed on the representative graphs, but instead serve to illustrate differences.

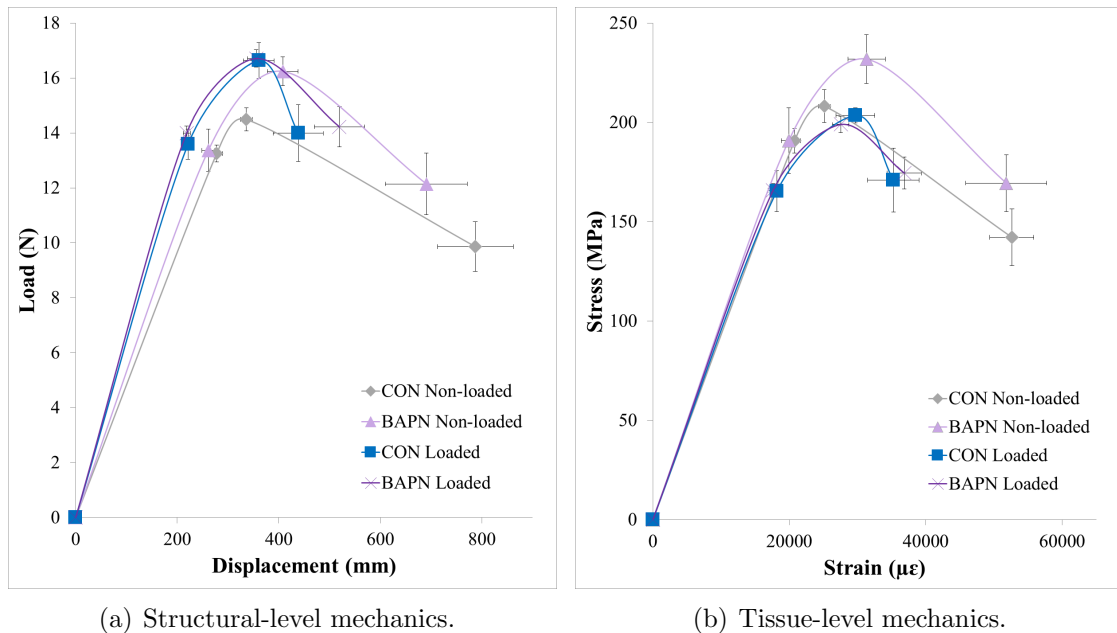


Fig. 3.5. Representative Force-Displacement and Stress-Strain curves show a robust response of load in terms of structure-level properties. When normalized by cross-sectional area, the effect of load is less pronounced. Treatment with BAPN had no effect on the mechanics.

Table 3.3.
Structural-level bone mechanical properties

Bone Property	CON		BAPN		Two-way ANOVA		
	Non-Loaded	Loaded	Non-Loaded	Loaded	Disease	Load	Interaction
Yield Force (N)	13.3 ± 1.0	13.6 ± 1.7	13.4 ± 2.4	14.0 ± 0.8			
Ultimate Force (N)	14.5 ± 1.3	16.6 ± 2.1	16.2 ± 1.6	16.7 ± 1.0	NS	0.01	NS
Disp to Yield (μm)	278 ± 37	221 ± 22	261 ± 39	219 ± 22	NS	<.0001	NS
Postyield Disp (μm)	507 ± 250	216 ± 158	424 ± 271	292 ± 142	NS	0.01	NS
Total Disp (μm)	787 ± 236	439 ± 155	691 ± 256	519 ± 157	NS	0.007	NS
Stiffness (N/mm)	54.1 ± 8.5	69.9 ± 8.9	57.9 ± 9.3	71.6 ± 12.7	NS	0.0007	NS
Work to Yield (mJ)	1.92 ± 0.14	1.67 ± 0.34	1.94 ± 0.51	1.75 ± 0.24	NS	NS	NS
Postyield Work (mJ)	5.47 ± 2.22	3.27 ± 2.29	5.54 ± 3.11	4.25 ± 1.65	NS	0.04	NS
Total Work (mJ)	7.48 ± 2.20	4.97 ± 2.30	7.56 ± 2.92	6.00 ± 1.69	NS	0.047	NS

^a Data are mean ± SD

Table 3.4.
Tissue-level bone mechanical properties

Bone Property	CON		BAPN		Two-way ANOVA		
	Non-Loaded	Loaded	Non-Loaded	Loaded	Disease	Load	Interaction
Yield Stress (MPa)	191 ± 20	165 ± 32	191 ± 53	166 ± 11	NS	NS	NS
Ultimate Stress (MPa)	208 ± 26	204 ± 12	232 ± 39	199 ± 13	NS	NS	NS
Strain to Yield (mε)	20.8 ± 2.7	18.2 ± 2.1	19.9 ± 3.3	17.6 ± 2.4	NS	0.02	NS
Total Strain (mε)	52.6 ± 10.2	35.3 ± 11.9	51.8 ± 18.8	36.9 ± 7.9	NS	0.01	NS
Modulus (GPa)	10.4 ± 2.0	10.6 ± 3.0	11.0 ± 3.5	11.4 ± 2.2	NS	NS	NS
Resilience (MPa)	2.16 ± 0.32	1.64 ± 0.31	2.09 ± 0.62	1.60 ± 0.19	NS	0.007	NS
Toughness (MPa)	7.31 ± 2.35	4.93 ± 2.34	7.60 ± 3.36	5.80 ± 1.83	NS	0.04	NS

^a Data are mean ± SD

From the load-displacement graph and table, it is clear that the loaded limbs were stiffer and able to maintain higher forces before breaking. However, once the data were normalized to the cross-sectional area, there was little effect of loading. Interestingly, the non-loaded BAPN mice had the greatest strength when normalized to cross-sectional area (although not significantly different than the other groups). In addition, although there were some effects of disease in the morphology of the tibiae, there were no effects of BAPN in terms of mechanics. These results are summarized in Tables 3.3 and 3.4.

3.4 Discussion

The results of this study showed some small effects of BAPN on tibial morphology that did not extend to mechanics. Tibial load offered some improvement in CON and BAPN mice. However, the improvements seemed to be driven primarily by an increase in mass and not due to improvements in bone quality.

3.4.1 Little Effect of BAPN Treatment

As seen in the previous study, the effects of BAPN were mild. There were some alterations in morphology, but none in mechanics, suggesting that a functional disease state was again not induced. However, while the effects of BAPN were mild in terms of morphology, BAPN altered the ability of the bone to respond to load. In CON mice, loading resulted in increased total cross-sectional area and periosteal bone surface, suggesting that load increased mass by periosteal expansion. In contrast, loading in the BAPN mice did not have increased total cross-sectional area or periosteal bone surface, but instead had decreased medullary area, suggesting that loading increased mass by endocortical contraction in the BAPN mice. In addition, loading caused a significant decrease in bone volume fraction in the BAPN mice, but not the CON mice. Taken together, these results suggest that, rather than having mechanical stimulation improve the BAPN-induced disease, BAPN altered some of

the effects of loading. Despite these observations, an overt disease phenotype was not produced, making it difficult to fully assess the effect of disease.

The dosage for these two studies was selected based on previous work showing a disease state with similar dosages [2,3]. The first study by McNerny et al. [2] showed decreased collagen cross-linking, altered bone morphology, and decreased fracture resistance in mice injected daily with 150 mg/kg and 350 mg/kg of BAPN. The second study, also by McNerny et al. [3], showed decreased mechanical properties, such as stiffness, yield force, and ultimate force, in BAPN mice. For that reason, it was thought that similar effects would be observed in mice in the current study. As noted, that was not the case. One cause of this disparity may be sex-based. In both studies by McNerny et al., male mice were used whereas in the current studies, female mice were employed. Another study, exploring the impact of lathyrism on aortas indicated that male mice were more often affected by the disease (i.e. more aortic aneurisms were observed) [4]. Despite this, we had chosen to use female mice due to the cage fighting that is often observed in male mice of this breed. In fact, Meakin et al. [5] showed that the amount of cage fighting in group housed males was sufficient to obscure the effect of tibial loading. Since a major goal of this study was to observe the effect of load, female mice were used. However, doing so may have inadvertently prevented the observation of a BAPN disease state.

Another potential limitation could be in the frequency of dosage. In the current studies, mice were injected with a bolus once a day. Thus, in order to impact the bone tissue, the BAPN would need to reach the bone tissue prior to clearance from the body. Depending on the rate of clearance, it is possible that a bolus injection was cleared from the body too quickly to have its full effect. To circumvent this problem, future studies could be conducted in which mice are injected multiple times per day. Alternatively, another mode of disease induction is drug dosing through the diet [6–8] which may have the added benefit of providing a more constant supply of the drug. Future studies will be directed toward inducing a disease state through this alternative method.

3.4.2 Robust Bone Formation Response Due to Loading

While there was little effect of disease, the response to load was robust in terms of bone mass and structural-level mechanical properties, but not in terms of tissue-level mechanical properties. In addition, even though the rest period during loading was kept at the high load, as done previously [1], the mice still showed signs of limping, though not nearly to the degree that was seen in the previous BAPN study (Chapter 2). For this reason, Chapter 4 explores the effect of various loading regimens on the pain of the mice during loading (as assessed by the degree of limping, stiff knees, and swollen ankles) with respect to the morphological and mechanical impacts of that loading. The goal is to prevent pain while inducing a bone formation response that results in improved morphology and mechanics.

3.5 Conclusion

Treatment of mice with a long-term high dose of BAPN was unable to induce mechanical alterations, and only mildly impacted the morphology. While the lack of effects could be sex-dependent, it could also be dependent on the fact the drug was provided as a bolus injection and may have been quickly cleared from the body, preventing induction of a disease. Future studies will be aimed at inducing a disease by alternate modes, such as through diet.

3.6 References

- [1] A. G. Berman, C. A. Clauser, C. Wunderlin, M. A. Hammond, and J. M. Wallace, “Structural and mechanical improvements to bone are strain dependent with axial compression of the tibia in female c57bl/6 mice,” *PloS one*, vol. 10, no. 6, p. e0130504, 2015.
- [2] E. M. B. McNerny, B. Gong, M. D. Morris, and D. H. Kohn, “Bone fracture toughness and strength correlate with collagen cross-link maturity in a dose-controlled lathyrism mouse model,” *Journal of Bone and Mineral Research*, vol. 30, no. 3, pp. 455–464, 2015. [Online]. Available: <http://dx.doi.org/10.1002/jbmr.2356>
- [3] E. M. B. McNerny, J. D. Gardinier, and D. H. Kohn, “Exercise increases pyridinoline cross-linking and counters the mechanical effects of concurrent lathyrogenic treatment,” *Bone*, vol. 81, pp. 327–337, 2015. [Online]. Available: <http://www.sciencedirect.com/science/article/pii/S875632821500304X>
- [4] H. M. McCallum, “Experimental lathyrism in mice,” *The Journal of pathology and bacteriology*, vol. 89, no. 2, pp. 625–636, 1965.
- [5] L. B. Meakin, T. Sugiyama, G. L. Galea, W. J. Browne, L. E. Lanyon, and J. S. Price, “Male mice housed in groups engage in frequent fighting and show a lower response to additional bone loading than females or individually housed males that do not fight,” *Bone*, vol. 54, no. 1, pp. 113–117, 2013.
- [6] E. P. Paschalis, D. N. Tatakis, S. Robins, P. Fratzl, I. Manjubala, R. Zoehrer, S. Gamsjaeger, B. Buchinger, A. Roschger, R. Phipps, A. L. Boskey, E. Dall’Ara, P. Varga, P. Zysset, K. Klaushofer, and P. Roschger, “Lathyrism-induced alterations in collagen cross-links influence the mechanical properties of bone material without affecting the mineral,” *Bone*, vol. 49, no. 6, pp. 1232–1241, 2011. [Online]. Available: <http://www.sciencedirect.com/science/article/pii/S8756328211011951>
- [7] J. Robinson and T. Bast, “Bone changes due to lathyrism in rats,” *The Anatomical Record*, vol. 59, no. 3, pp. 283–295, 1934.
- [8] B. J. Geiger, H. Steenbock, and H. T. Parsons, “Lathyrism in the rat,” *J Nutr*, vol. 6, pp. 427–442, 1933.

4. MODIFYING PARAMETERS AND SCHEDULE DURING AXIAL COMPRESSION OF THE MURINE TIBIA INCREASES BONE TISSUE QUALITY AND QUANTITY AND DECREASES ANIMAL DISCOMFORT

4.1 Introduction

Axial compression of the tibia is a commonly used technique to assess the response of bone to mechanical loading in a controlled environment [1]. Although mice tolerate the loading well, they frequently show signs of discomfort (i.e. limping) immediately following a loading bout. Although the mice are typically recovered within an hour, the primary goal of this study was to assess alternate loading profiles that reduce pain while still maintaining a robust bone formation response to loading.

The resistance of a bone to fracture is dependent on a number of factors that can be broadly divided into three main contributors: bone mass, bone structure, and bone quality. Although all three are necessary for proper bone mechanical integrity, the typical metric used clinically to assess fracture risk is bone mineral density measured using dual-energy X-ray absorptiometry (DXA) [2,3], which only accounts for bone mass and structure. Moreover, the efficacy of clinical treatments for bone diseases is often dependent on the ability of the treatment to increase bone mineral density, and not in its ability to reduce fracture risk (often difficult to assess). Even in pre-clinical models, outcomes of a specific treatment regime are often restricted to measures of structure, mass, or both. While increasing mass and improving structure are good outcomes, and many valuable studies have been conducted investigating such endpoints, it is important that quality of the tissue also be explored. These quality based functional bone outcomes often cannot be tested in clinical studies. In contrast, pre-clinical models provide a prime opportunity to assess the impact of a

treatment on bone quality, enabling greater understanding of how a treatment might contribute to bone mechanical integrity. A secondary goal of this study was to assess how the different loading regimens affect bone quality.

One potential treatment for bone defects and disease that is heavily studied is bone adaption through mechanical stimulation. Both clinical and pre-clinical studies have shown beneficial effects of exercise on bone mass [4–7]. To explore a more controlled response to load, targeted loading models have also been employed such as tibial four-point bending [8], ulnar loading [9, 10], and tibial axial compression [1]. Like the exercise models, these targeted loading models have been shown to beneficially affect bone mass in pre-clinical models [11, 12]. However, the role of these treatments on bone quality is less clearly defined. Some studies have shown exercise and targeted loading-based improvements in post-yield mechanical properties [13, 14] and in fatigue properties [15, 16]. In contrast, a different study showed a lack of effect on bone quality as assessed by ultimate strength [17]. This dichotomy of results indicates that further research is needed to understand what types of mechanical stimulation cause quality-based improvements to bone.

A previous study in our lab indicated that although the tibia shows robust improvements in bone mass to targeted axial compression, those results may be decoupled from quality-based improvements as assessed by fracture toughness testing (data unpublished). One hypothesis was that limping observed immediately following loading was a sign of injury and that the injury caused the body to rapidly lay down more bone, to the negligence of the tissue quality. The goal of this study was therefore two-fold: 1) To reduce pain in the animals as assessed by limping, joint stiffness, and ankle swelling and 2) To understand the role of mechanical stimulation on bone quantity and quality as assessed by computed tomography and fracture toughness, respectively.

4.2 Methods

4.2.1 Animals

Twenty-three female C57Bl6 mice (Envigo) were obtained at 7 weeks of age and allowed to acclimate for one week prior to the start of the study. At eight weeks of age, mice were separated into 4 weight matched groups: MoTuWe High (n = 5; 18.1 ± 0.5 g), MoTuWe Low (n = 6; 17.8 ± 0.7 g), MoWeFr Low (n = 6; 17.8 ± 0.7 g), and TuFr Low (n = 6; 17.7 ± 1.2 g). Mice were then weighed on every day of loading to assess animal health. All animal procedures were performed with prior approval from the Indiana University School of Science Institutional Animal Care and Use Committee (IACUC).

4.2.2 *In vivo* Loading

For all groups, the right tibiae of the mice were loaded over a three week period. An example of a mouse limb within the tibial loading fixture is shown in Figure 4.1.

The specific days of loading are indicated in the groups name (MoTuWe was loaded on Monday, Tuesday and Wednesday of each week, etc.). For all mice, the contralateral limb acted as an internal, non-loaded control. Each loading bout consisted of 4 loading cycles at 2 Hz followed by 3 seconds of rest, repeated 55 times for a total of 220 loading cycles. All mice were loaded to a peak compressive load of 10.6 N (engendering $2050 \mu\epsilon$ [18]). The Low groups were held at 2 N for the 3 second rest period, while the High group was held at 10.6 N for the rest period. A summary of the groups is found in Table 4.1.

Following each loading bout, mice were assessed for limping on a scale of 0 (no limping) to 5+ (limping that does not recover). Table 4.2 explains the various levels.

Throughout the study, at a minimum, all mice were able to recover and walk using both limbs by the following day. However, by week 3, mice in the MoTuWe High group had swollen ankles that did not subside by the next day. That, in conjunction

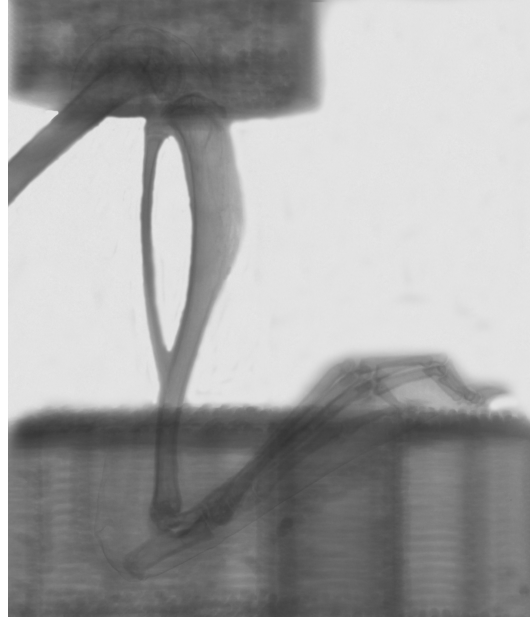


Fig. 4.1. Representative ex vivo μ CT scan of a mouse limb in the tibial loading fixture shows the orientation of the limb during loading.

Table 4.1.
Summary of Groups

	Number of mice	Number of days loaded each week	Maximum Load	Load during rest
MoTuWe High	5	3	10.6 N	10.6 N
MoTuWe Low	6	3	10.6 N	2 N
MoWeFr	6	3	10.6 N	2 N
TuFr	6	2	10.6 N	2 N

with the continuous severity of limping following loading led to the decision not to load the mice on the final 2 days. In addition, there were two mice in the MoTuWe Low group which also had swollen ankles that did not subside by the next day and therefore, were not loaded (one mouse for the final day and the second mouse for the final two days). Despite swollen ankles, the mice used both limbs while walking and the mice continued to gain weight over the duration of the study.

Table 4.2.
Limping Assessment Scale

0	No Limp
1	Mild Limp; Will use both feet, but slight preference for the non-loaded contralateral limb
2	Mild to Moderate; Will use both feet, but noticeable preference for the non-loaded contralateral limb
3	Moderate; Will use both feet, but hobbles on the loaded limb
4	Moderate to Severe; May or may not touch with loaded limb, but not use; Uses both limbs within 1 hr of loading
5	Severe; May or may not touch with loaded limb, but not use; Limp remains after 1 hr, but mouse is recovered by next day.
5+	Limping that does not recover by the next day

At 11 weeks of age, all mice were euthanized by CO₂ asphyxiation. Immediately after euthanasia, all mice were checked for swollen ankles and stiff knees, and were ranked for each on a scale of 0–2, with a “0” implying no observable signs and a “2” implying severe. After assessment, the right and left limbs (femur/tibia/foot complex) were removed and stored at 4 °C until scanning by micro computed tomography (μ CT), which occurred within 24 hr. After scanning, the tibiae were harvested, wrapped in saline-soaked gauze, and stored at -20 °C until fracture toughness testing.

4.2.3 Micro Computed Tomography (μ CT)

The right and left limbs were scanned while hydrated at 8.4 μ m resolution using a μ CT system (Bruker Skyscan 1176). Calibration was performed using two hydroxypatite phantoms at 0.25 and 0.75 g/cm³ in order to convert the grayscale images into mineral density. Images were then reconstructed for cortical analyses.

For cortical analysis, a region of interest (ROI) was selected as seven transverse slices centered at 50% of the bone length. Tissue mineral density (TMD) was calculated and then a binary threshold was applied and geometric properties were calculated using a custom MATLAB code.

4.2.4 Fracture Toughness Testing

Following μ CT, the tibiae were tested to assess fracture toughness [19,20]. Prior to mechanical testing, tibiae were hand-notched with a scalpel blade in the medial region of the mid-diaphysis, proximal to the tibia-fibula junction. During notching, the scalpel blade was lubricated with a 1 μ m diamond suspension. The notch entered the medullary cavity but did not proceed more than halfway through the bone. After notching, bones were tested to failure in three-point bending at 0.001 mm/sec with the notched side in tension and the notch located directly under the applied load. After the test, μ CT images were pulled from an ROI located 1 mm above the tibula-fibula junction (notch location) and used to determine geometric properties at the location of fracture. Bones were then dehydrated with graded ethanol (70–100%), and the fracture surface was imaged using scanning electron microscopy (SEM). Images obtained were used to determine the angles of stable and unstable crack growth. Force and displacement data, geometric properties, and the crack growth angles were used in a custom MATLAB script to determine fracture stress intensity (K) values at yield force (crack initiation), at maximum force, and at failure force (crack instability).

4.2.5 Statistics

For body weight, one-way ANOVA was used. For all other analyses, paired t-tests were performed to assess the difference between the loaded and non-loaded limbs within each group. The data were checked for assumptions of normality and homogeneity of variance. In the case of assumption violations, a Mann Whitney U test was performed instead of the paired t-test.

4.3 Results

4.3.1 *In vivo* Assessment

Throughout the study, mice continued to gain weight and groom themselves normally. At the start of the study, mouse weights were 18.1 ± 0.5 g for MoTuWe High; 17.8 ± 0.7 g for MoTuWe Low; 17.8 ± 0.7 g for MoWeFr; and 17.7 ± 1.2 g for TuFr groups. At the end of study, mouse weights were 19.3 ± 0.4 g for MoTuWe High; 18.6 ± 0.6 g MoTuWe Low; 18.3 ± 0.9 g for MoWeFr; and 19.1 ± 1.3 g for TuFr groups. There were no significant differences between groups.

However, the number of days loaded and load applied during the rest period both severely impacted each mouse's pain response, as assessed by observing the degree of limping after each loading bout, as well as by noting the degree of knee stiffening and ankle swelling at the end of the study.

Throughout the study, the mice in the MoTuWe High group had a greater degree of limping than the other groups. This was followed by the MoTuWe Low group, and then by the MoWeFr group, with the TuFr group showing none to mild signs of limping throughout the study (Tables 4.3, 4.4, and 4.5).

Table 4.3.
Limping Assessment Week 1

	Week 1				
	Day 1	Day 2	Day 3	Day 4	Day 5
MoTuWe High	1.0 (0, 2)	3.0 (2, 3)	4.0 (4, 5)		
MoTuWe Low	0.0 (0, 0)	0.5 (0, 3)	2.0 (1, 5)		
MoWeFr	0.0 (0, 1)		1.5 (0, 2)		2.0 (1, 2)
TuFr		0.0 (0, 0)			1.0 (0, 1)

Data are median and range (in parentheses) of limping observed in the mice after each day of loading. On the scale, a “1” suggests mild limping described as a slight preference of the non-loaded limb, a “3” is moderate limping, and a “5+” is severe limping that does not recover by the following day.

Table 4.4.
Limping Assessment Week 2

	Day 1	Day 2	Day 3	Day 4	Day 5
MoTuWe High	3.0 (3, 4)	4.0 (4, 4)	4.0 (4, 4)		
MoTuWe Low	0.0 (0, 2)	1.0 (1, 4)	1.0 (1, 4)		
MoWeFr	1.0 (0, 1)		1.0 (0, 2)		1.0 (1, 2)
TuFr		0.0 (0, 0)			0.0 (0, 1)

Data are median and range (in parentheses) of limping observed in the mice after each day of loading. On the scale, a “1” suggests mild limping described as a slight preference of the non-loaded limb, a “3” is moderate limping, and a “5+” is severe limping that does not recover by the following day.

Table 4.5.
Limping Assessment Week 3

	Day 1	Day 2	Day 3	Day 4	Day 5
MoTuWe High	4.0 (3, 5)				
MoTuWe Low	1.5 (0, 2)	2.0 (0, 3)	1.5 (1, 3)		
MoWeFr	1.5 (1, 2)		1.0 (1, 2)		2.0 (1, 2)
TuFr		0.0 (0, 1)			0.0 (0, 1)

Data are median and range (in parentheses) of limping observed in the mice after each day of loading. On the scale, a “1” suggests mild limping described as a slight preference of the non-loaded limb, a “3” is moderate limping, and a “5+” is severe limping that does not recover by the following day.

To better assess the information, the data from each mouse’s last day of loading was used to create Table 4.6 and Figure 4.2. It is clear from both the figure and the table that the limping was greatest in the MoTuWe High group, followed by the MoTuWe Low group, the MoWeFr group, and finally, the TuFr group.

The assessment of knee stiffening and ankle swelling corroborated with the assessment of limping, as shown in Tables 4.7 and 4.8.

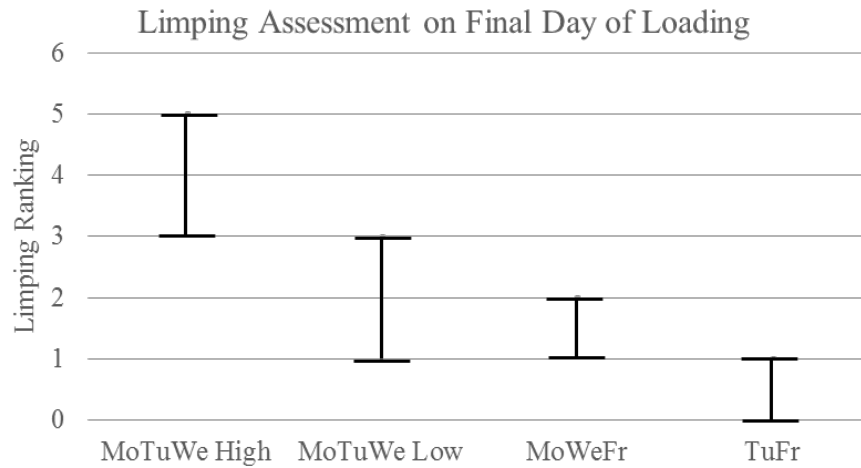


Fig. 4.2. The range of limping observed in the mice after the final day of loading clearly demonstrate that the MoTuWe High group had increased limping as compared to the other groups.

Table 4.6.
Count of mice at each limping level after the final day of loading.

	0	1	2	3	4	5	5+
MoTuWe High				1	3	1	
MoTuWe Low		2	2	2			
MoWeFr		2	4				
TuFr	5	1					

Table 4.7.
Joint stiffness at the end of the study.

	0	1	2
MoTuWe High		2	3
MoTuWe Low	1	3	2
MoWeFr	3	2	1
TuFr	6		

Table 4.8.
Swollen ankle assessment at the end of the study.

	0	1	2
MoTuWe High	2		3
MoTuWe Low	4	1	1
MoWeFr	2	4	
TuFr	6		

Altogether, the three assessments of pain all suggest that holding at the high load level is detrimental to the mice. In addition, holding at the low load level, but loading multiple days in a row also seems to negatively impact the mice. The least detriment was caused by loading only twice a week and holding at the low load level.

4.3.2 CT Whole Limb Assessment

After euthanasia, the limbs from each mouse were removed and scanned to assess the whole femur/tibia/foot complex. While the assessment of limping in vivo suggested that the mice were uncomfortable with loading, all recovered by the following day and were able to use both limbs while walking. Thus, while it was expected that the MoTuWe High group would have some degree of altered bone morphology, the degree of damage observed in MoTuWe High and MoTuWe Low group was unexpected. Figures 4.3, 4.4, 4.5, and 4.6 show the CT shadow scans of the loaded limbs for each group, with the pain assessment scores on the final day of loading noted for each animal.

Clear damage is observed in the MoTuWe High and MoTuWe Low groups. In the MoTuWe High group, two mice had broken fibulas and crushed proximal metaphyses. Moreover, there were two additional mice which had damaged epiphyses. The MoTuWe Low group also showed signs of damage, though not as severe. The fibula was broken in one mouse and the proximal metaphysis deformed in two of the mice.

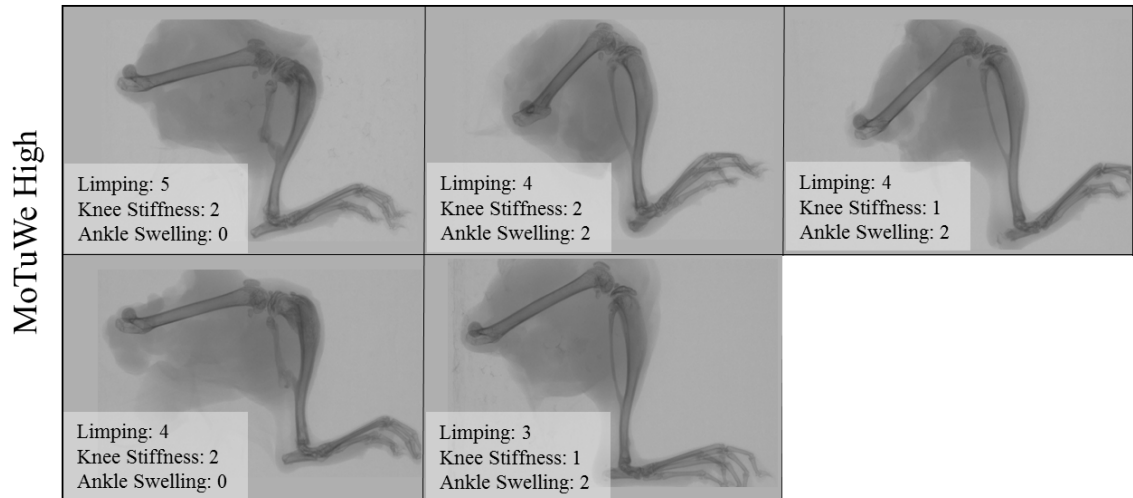


Fig. 4.3. Scout scans of the MoTuWe High group show clear damage. The fibula is broken and the proximal metaphysis deformed in two of the mice. In addition, the epiphysis appears deformed in an additional two mice. Due to swollen ankles and limping after loading, the MoTuWe High group was not loaded on the last two days.

In addition, the epiphysis appears deformed in an additional mouse. In contrast, the MoWeFr and TuFr groups did not show overt signs of damage in the uCT shadow scans. These results agree with the assessment of pain, discussed previously.

4.3.3 Cortical Analysis

The graded response in terms of limping, swelling, and knee stiffening was also seen in the cortical analysis, shown in Figure 4.7.

Figure 4.7 demonstrates a robust, but graded, response in the four loading groups. All four groups showed significant periosteal expansion resulting in increased cortical area and thickness. However, the MoTuWe High group demonstrated the greatest bone formation effect, while the TuFr group showed the least. Although this graded response was true for most parameters, it is interesting to note that the MoWeFr

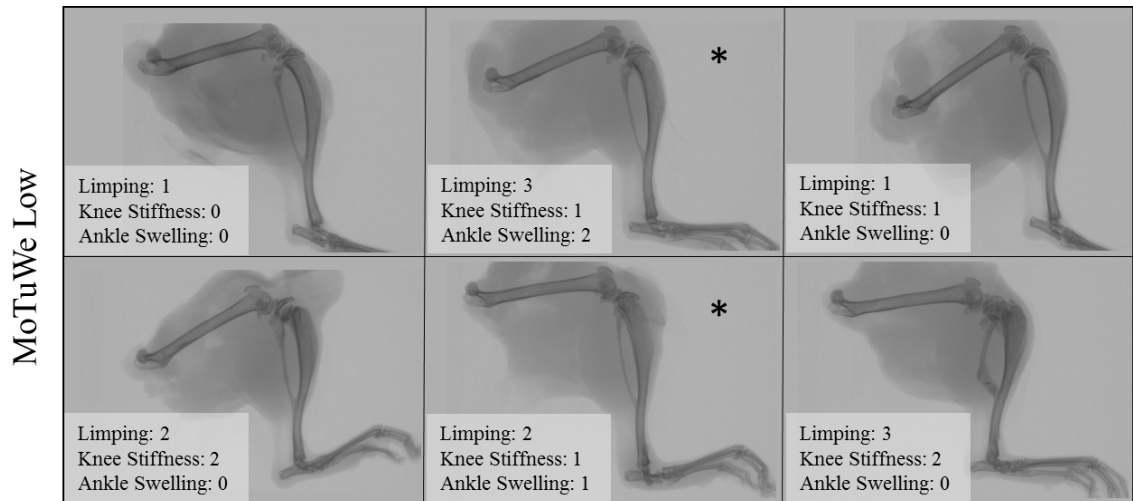


Fig. 4.4. Scout scans of the MoTuWe Low group also show damage. The fibula is broken in one mouse and the proximal metaphysis deformed in two of the mice. In addition, the epiphysis appears deformed in an additional mouse. Two mice (indicated by the “*”) did not complete the loading regimen due to the assessment of pain.

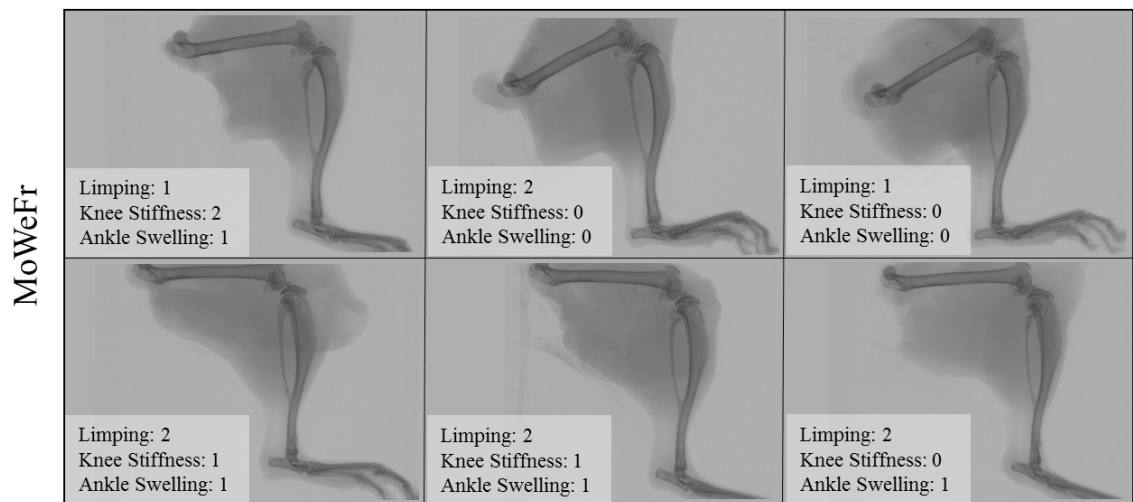


Fig. 4.5. Scout scans of the MoWeFr group lack the damage observed in the MoTuWe High and MoTuWe Low groups. All mice were able to be loaded the length of the study.

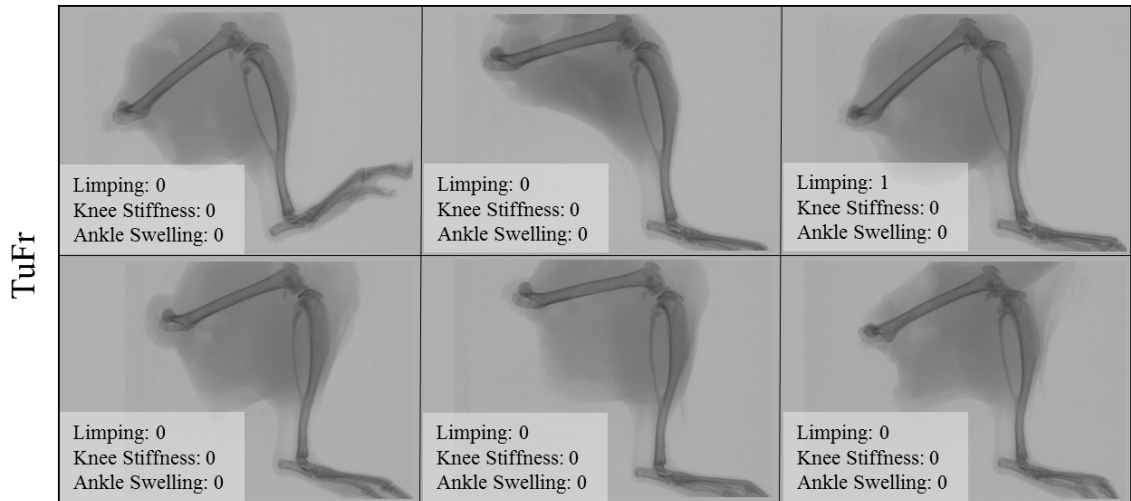


Fig. 4.6. Scout scans of the TuFr group lack the damage observed in the MoTuWe High and MoTuWe Low groups. All mice were able to be loaded the length of the study.

and TuFr groups had increased tissue mineral density, whereas the MoTuWe High and MoTuWe Low groups did not (Tables 4.9 and 4.10).

Interestingly, although the MoTuWe High group had greater mass than the other three groups, the increased amount of injury (as determined by increased assessment of pain) seemed to result in greater variability among the mice, leading to much larger standard deviations for the cortical geometric parameters. A clear depiction of the graded response and the high variability can be observed in the graph of cortical thickness (Figure 4.8).

4.3.4 Fracture Toughness Testing

Fracture toughness, an assessment of bone quality, was also performed on the tibiae (Figure 4.9).

Although few properties showed significant differences with loading, Figure 4.9 shows clear trends toward increased fracture resistance in the MoTuWe Low and MoWeFr groups across all three stress intensity measures. In contrast, the MoTuWe

Table 4.9.
Cortical morphology assessed by μ CT (MoTuWe High and MoTuWe Low groups)

Bone Property	MoTuWe High		MoTuWe Low	
	Non-Loaded	Loaded	Non-Loaded	Loaded
tCSA (mm ²)	0.903 ± 0.029	1.004 ± 0.092*	0.883 ± 0.025	0.956 ± 0.028*
Med.Ar (mm ²)	0.361 ± 0.021	0.343 ± 0.042	0.354 ± 0.019	0.327 ± 0.032
Ct.Ar (mm ²)	0.543 ± 0.010	0.661 ± 0.125*	0.529 ± 0.015	0.629 ± 0.020*
Ct.Th (mm)	0.197 ± 0.004	0.234 ± 0.043*	0.193 ± 0.006	0.228 ± 0.011*
pBS (mm)	4.120 ± 0.051	4.308 ± 0.152*	4.052 ± 0.047	4.211 ± 0.058*
eBS (mm)	2.705 ± 0.065	2.638 ± 0.192	2.684 ± 0.060	2.560 ± 0.116 [^]
Iap (mm ⁴)	0.051 ± 0.005	0.066 ± 0.015	0.050 ± 0.003	0.059 ± 0.002*
Iml (mm ⁴)	0.062 ± 0.003	0.083 ± 0.020*	0.058 ± 0.004	0.075 ± 0.006*
TMD (g/cm ³)	1.151 ± 0.008	1.158 ± 0.011	1.153 ± 0.006	1.168 ± 0.028

^a Data are mean ± SD

^b tCSA = total cross sectional area; Med.Ar = medullary area; Ct.Ar = cortical area;

Ct.Th = cortical thickness; pBS = periosteal bone surface; eBS = endocortical bone surface; Iap = moment of inertia about the anterior-posterior axis; Iml = moment of inertia about the medial-lateral axis; TMD = tissue mineral density

* p < 0.05 vs non-loaded limb within same group (paired t-test or Mann-Whitney U test)

[^] p < 0.1 vs non-loaded limb within same group (paired t-test or Mann-Whitney U test)

Table 4.10.
Cortical morphology assessed by μ CT (MoWeFr and TuFr groups)

Bone Property	MoTuWe High		MoTuWe Low	
	Non-Loaded	Loaded	Non-Loaded	Loaded
tCSA (mm ²)	0.878 ± 0.048	0.941 ± 0.047*	0.896 ± 0.071	0.930 ± 0.056 [^]
Med.Ar (mm ²)	0.345 ± 0.039	0.319 ± 0.048 [^]	0.357 ± 0.038	0.340 ± 0.026
Ct.Ar (mm ²)	0.533 ± 0.018	0.622 ± 0.023*	0.539 ± 0.038	0.590 ± 0.042*
Ct.Th (mm)	0.196 ± 0.007	0.227 ± 0.014*	0.196 ± 0.008	0.213 ± 0.011*
pBS (mm)	4.043 ± 0.118	4.195 ± 0.093*	4.082 ± 0.157	4.175 ± 0.103*
eBS (mm)	2.631 ± 0.169	2.567 ± 0.202	2.668 ± 0.154	2.617 ± 0.103
Iap (mm ⁴)	0.049 ± 0.006	0.057 ± 0.006*	0.051 ± 0.007	0.054 ± 0.007*
Iml (mm ⁴)	0.059 ± 0.005	0.075 ± 0.008*	0.061 ± 0.010	0.072 ± 0.009*
TMD (g/cm ³)	1.163 ± 0.015	1.188 ± 0.019*	1.154 ± 0.007	1.169 ± 0.014*

^a Data are mean ± SD

^b tCSA = total cross sectional area; Med.Ar = medullary area; Ct.Ar = cortical area;

Ct.Th = cortical thickness; pBS = periosteal bone surface; eBS = endocortical bone surface; Iap = moment of inertia about the anterior-posterior axis; Iml = moment of inertia about the medial-lateral axis; TMD = tissue mineral density

* p < 0.05 vs non-loaded limb within same group (paired t-test or Mann-Whitney U test)

[^] p < 0.1 vs non-loaded limb within same group (paired t-test or Mann-Whitney U test)

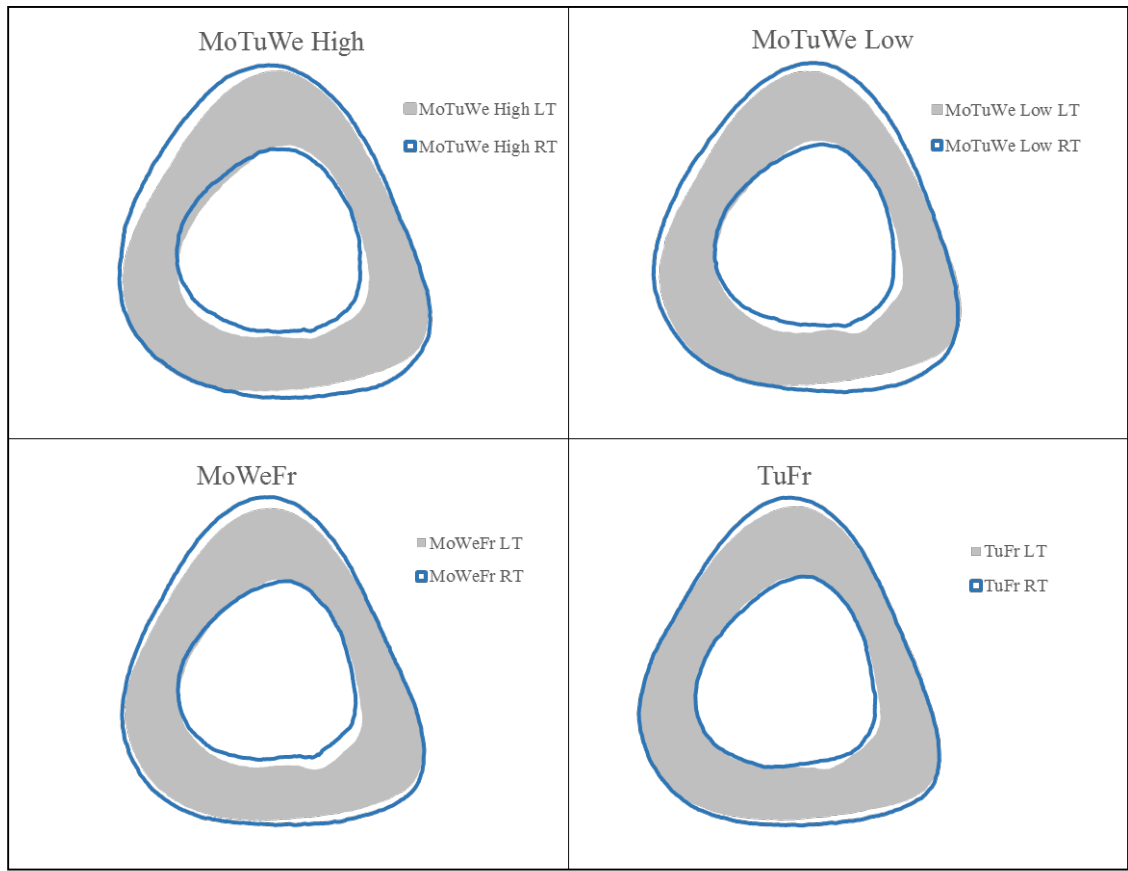


Fig. 4.7. Cortical cross-sectional areas in each of the groups shows an increase in bone mass in response to load.

High group only shows an upward trend in fracture toughness at crack instability, and the TuFr group show no upward trend across any of the stress intensity measures.

4.4 Discussion

The primary aim of this study was to be able to reduce pain during loading while still maintaining a robust bone formation effect. The pain observed in the MoTuWe High group, and the slightly lesser pain observed in the MoTuWe Low group, clearly demonstrate that holding the load at the high load level during rest and decreasing the number of rest days between loading bouts will cause increased pain in the mice.

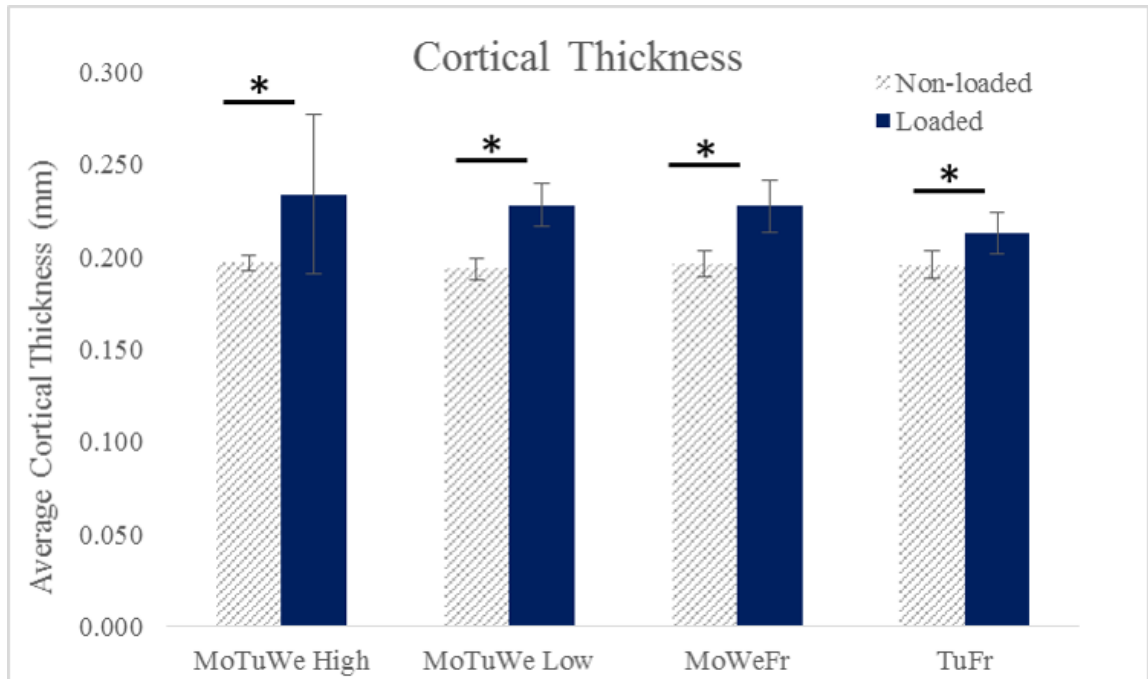
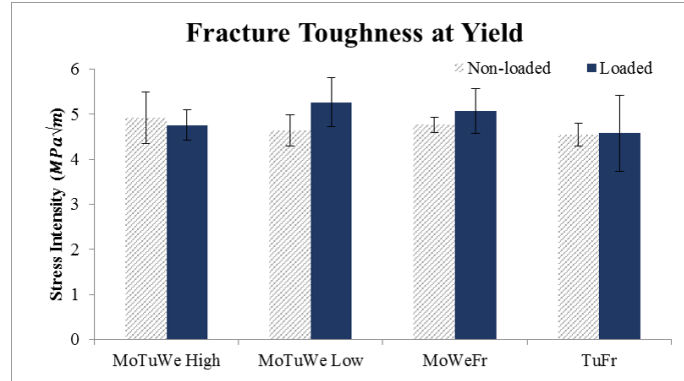


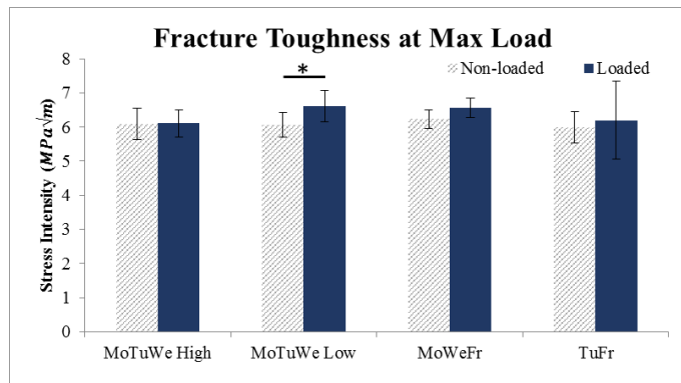
Fig. 4.8. Cortical thickness demonstrates the graded response due to loading in the four groups. MoTuWe High group had the greatest effect, followed by MoTuWe Low, MoWeFr, and lastly, TuFr. Interestingly, the MoTuWe High group also had increased variability. Significant differences ($p < 0.05$) are indicated by an “*”.

The MoTuWe group held at the high load level experienced greater limping, more swollen ankles, and stiffer joints than any of the other groups. In addition, the μ CT shadow scans clearly showed damage in the tibia and fibula in that group. This resulted in a large, but variable, bone formation response. Although increased bone mass likely contributed to increased mechanical integrity of the bones, there was little effect on fracture toughness and no effect of mineral density as assessments of bone quality/material properties. Therefore, despite the beneficial effect of loading on bone formation, this loading profile did not improve bone quality and caused greater pain in the animals.

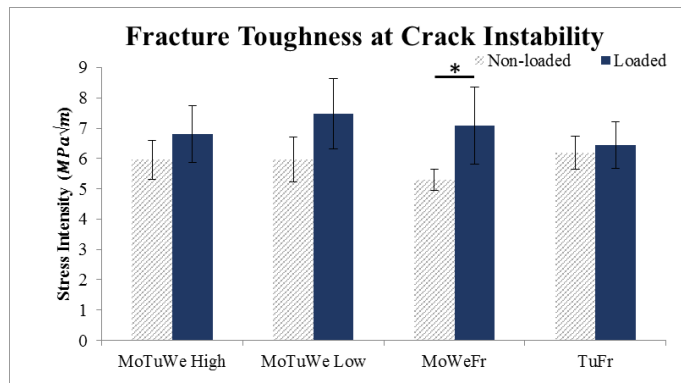
These results in terms of limping are in contrast to previously published work which only noted limping at a higher force/strain level and not at the force/strain



(a) Fracture toughness at crack initiation.



(b) Fracture toughness at maximum load.



(c) Fracture toughness at crack instability

Fig. 4.9. Graphs of fracture toughness parameters showing increasing crack stress intensity in the MoTuWe Low and MoWeFr groups at (a) yield force (crack initiation), (b) maximum force and (c) failure force (crack instability). Significant differences ($p < 0.05$) are indicated by an “*”.

level used in this study [18]. The mice in that study were purchased from the same vendor and were of the same breed, sex, and age. However, those mice weighed significantly more than the mice in this study (17.8 ± 0.8 g in the current study as compared to 18.8 ± 0.9 g in the previous study). The larger mice in the previous cohort may have been better able to handle the load without limping, suggesting that the amount of loading that a mouse can receive may be dependent on its size/mass, independent of its age.

In contrast to the MoTuWe High group, the TuFr group showed little to no pain throughout the study. Assessment of morphology still demonstrated increased cortical bone, though not to the degree observed in the other groups. Interestingly, loading in the TuFr group also had no effect on fracture toughness. These results suggest that while the loading stimulus in this group was enough to increase bone mass, it was insufficient to alter bone tissue quality.

Given the response in cortical structure in the TuFr group, it is possible that a longer-term study would improve fracture toughness. Unlike the other three groups, the TuFr group only received 6 total loading bouts over the 3 week period instead of the typical 9 bouts received by the other groups. It is possible that although the mice were loaded over the same total period of time (3 weeks), the decreased number of loading bouts was insufficient for a quality-based improvement. A longer study may be able to cause quality-based changes to bone without inducing the pain observed in the other groups. In other instances when quality outcomes are not of interest, use of a 2 day/week loading schedule is desirable due to the lack of limping observed.

The other two loading groups, MoTuWe Low and MoWeFr, both showed robust improvements in cortical morphology and upward trends in the three fracture toughness parameters. Of those two groups, the MoTuWe Low group demonstrated a greater degree of limping and a greater number of stiff knees. In addition, as was the case for the MoTuWe High group, the uCT shadow scans from the MoTuWe Low group demonstrated damage (at least one fractured fibula and 2 displaced proximal metaphyses in the tibia). Although less severe than the MoTuWe High group, these

types of injuries must be avoided. In contrast, the MoWeFr group showed mild to mild-moderate pain over the course of the study and no signs of damage in the CT shadow scans. While limping did occur, the mice still used both limbs for walking immediately after loading. The mild to mild-moderate assessment of pain indicated that mice had a slight to noticeable preference for the contralateral limb. Since the MoWeFr mice used both limbs for walking and only showed mild signs of pain, use of a MoWeFr loading regimen might be ideal for quantity and quality-based improvements. Future studies will explore the potential of decreasing the number of cycles during an individual loading bout to further reduce pain. Despite this, the minimal pain and improved bone structure and fracture toughness parameters observed in the MoWeFr group suggest that loading MoWeFr is best able to reduce pain while still maintaining a response in bone quantity and quality.

The primary limitation of this study was the low sample size. Since the primary goal of this study was to reduce pain during loading, a low sample size was selected for the current study with the intention of increasing sample size in future studies after an optimum loading schedule had been determined. However, doing so decreased the ability to observe differences in the fracture toughness parameters, resulting in clear trends, but few significant differences. The clear trends would suggest that loading was able to improve bone quality as assessed by fracture toughness in the MoTuWe Low and MoWeFr groups.

4.5 Conclusion

The concept of pain and its role in bone formation should not be ignored. The original hypothesis of this study was that the pain induced by loading would cause robust responses in cortical bone, but lack the desired effect on bone quality, as assessed by fracture toughness. This was certainly observed in the MoTuWe High group. However, the prevention of the bone from responding with quality-based improvements must require a high degree of injury because the MoTuWe Low group

also showed significant signs of pain, but were able to improve fracture toughness parameters. The only group to show no or little pain was the TuFr group, but loading in these mice had only modest (but significant) effects on cortical structure and no effects on fracture toughness. Due to the lack of limping in these mice, when quality-based effects are not assessed, the TuFr schedule would be a beneficial regime. Altogether, the MoWeFr group was best able to reduce pain while still maintaining a response in bone quantity and quality.

4.6 Acknowledgments

We would like to acknowledge the Integrated Nanosystems Development Institute for use of their JSM-7800F system, which was awarded through the National Science Foundation MRI-1229514 grant.

4.7 References

- [1] R. L. De Souza, M. Matsuura, F. Eckstein, S. C. F. Rawlinson, L. E. Lanyon, and A. A. Pitsillides, “Non-invasive axial loading of mouse tibiae increases cortical bone formation and modifies trabecular organization: A new model to study cortical and cancellous compartments in a single loaded element,” *Bone*, vol. 37, no. 6, pp. 810–818. [Online]. Available: <http://dx.doi.org/10.1016/j.bone.2005.07.022>
- [2] A. El Maghraoui and C. Roux, “Dxa scanning in clinical practice,” *Qjm*, vol. 101, no. 8, pp. 605–617, 2008.
- [3] G. M. Blake and I. Fogelman, “The role of dxa bone density scans in the diagnosis and treatment of osteoporosis,” *Postgraduate medical journal*, vol. 83, no. 982, pp. 509–517, 2007.
- [4] A. L. Huddleston, D. Rockwell, D. N. Kulund, and R. B. Harrison, “Bone mass in lifetime tennis athletes,” *JAMA*, vol. 244, no. 10, pp. 1107–9, 1980. [Online]. Available: <http://www.ncbi.nlm.nih.gov/pubmed/7411762>
- [5] P. C. Jacobson, W. Beaver, S. A. Grubb, T. N. Taft, and R. V. Talmage, “Bone density in women: college athletes and older athletic women,” *J Orthop Res*, vol. 2, no. 4, pp. 328–32, 1984. [Online]. Available: <http://www.ncbi.nlm.nih.gov/pubmed/6335524>
- [6] C. S. Duncan, C. J. Blimkie, C. T. Cowell, S. T. Burke, J. N. Briody, and R. Howman-Giles, “Bone mineral density in adolescent female athletes: relationship to exercise type and muscle strength,” *Med Sci Sports Exerc*, vol. 34, no. 2, pp. 286–94, 2002. [Online]. Available: <http://www.ncbi.nlm.nih.gov/pubmed/11828239>
- [7] J. Iwamoto, J. K. Yeh, and J. F. Aloia, “Differential effect of treadmill exercise on three cancellous bone sites in the young growing rat,” *Bone*, vol. 24, no. 3, pp. 163–169, 1999. [Online]. Available: <http://www.sciencedirect.com/science/article/pii/S8756328298001896>
- [8] C. H. Turner, M. P. Akhter, D. M. Raab, D. B. Kimmel, and R. R. Recker, “A noninvasive, in vivo model for studying strain adaptive bone modeling,” *Bone*, vol. 12, no. 2, pp. 73–79, 1991. [Online]. Available: <http://www.sciencedirect.com/science/article/pii/8756328291900032>
- [9] A. G. Torrance, J. R. Mosley, R. F. Suswillo, and L. E. Lanyon, “Noninvasive loading of the rat ulna in vivo induces a strain-related modeling response uncomplicated by trauma or periosteal pressure,” *Calcif Tissue Int*, vol. 54, no. 3, pp. 241–7, 1994. [Online]. Available: <http://www.ncbi.nlm.nih.gov/pubmed/8055374>
- [10] K. C. Lee, A. Maxwell, and L. E. Lanyon, “Validation of a technique for studying functional adaptation of the mouse ulna in response to mechanical loading,” *Bone*, vol. 31, no. 3, pp. 407–12, 2002. [Online]. Available: <http://www.ncbi.nlm.nih.gov/pubmed/12231414>

- [11] C. H. Turner, M. R. Forwood, J. Y. Rho, and T. Yoshikawa, "Mechanical loading thresholds for lamellar and woven bone formation," *Journal of Bone and Mineral Research*, vol. 9, no. 1, pp. 87–97, 1994. [Online]. Available: <http://dx.doi.org/10.1002/jbmr.5650090113>
- [12] C. T. Rubin and L. E. Lanyon, "Regulation of bone mass by mechanical strain magnitude," *Calcified Tissue International*, vol. 37, no. 4, pp. 411–417, 1985. [Online]. Available: <http://dx.doi.org/10.1007/BF02553711>
- [13] J. M. Wallace, R. M. Rajachar, M. R. Allen, S. A. Bloomfield, P. G. Robey, M. F. Young, and D. H. Kohn, "Exercise-induced changes in the cortical bone of growing mice are bone and gender specific," *Bone*, vol. 40, no. 4, pp. 1120–1127, 2007. [Online]. Available: <http://www.ncbi.nlm.nih.gov/pmc/articles/PMC2729655/>
- [14] J. M. Wallace, M. S. Ron, and D. H. Kohn, "Short-term exercise in mice increases tibial post-yield mechanical properties while two weeks of latency following exercise increases tissue-level strength," *Calcified tissue international*, vol. 84, no. 4, pp. 297–304, 2009.
- [15] S. J. Warden, R. K. Fuchs, A. B. Castillo, I. R. Nelson, and C. H. Turner, "Exercise when young provides lifelong benefits to bone structure and strength," *Journal of Bone and Mineral Research*, vol. 22, no. 2, pp. 251–259, 2007. [Online]. Available: <http://dx.doi.org/10.1359/jbmr.061107>
- [16] D. H. Kohn, N. D. Sahar, J. M. Wallace, K. Golcuk, and M. D. Morris, "Exercise alters mineral and matrix composition in the absence of adding new bone," *Cells Tissues Organs*, vol. 189, no. 1-4, pp. 33–7, 2009. [Online]. Available: <http://www.ncbi.nlm.nih.gov/pubmed/18703871>
- [17] L. Mosekilde, C. Danielsen, C. Sgaard, and E. Thorling, "The effect of long-term exercise on vertebral and femoral bone mass, dimensions, and strength assessed in a rat model," *Bone*, vol. 15, no. 3, pp. 293–301, 1994.
- [18] A. G. Berman, C. A. Clauser, C. Wunderlin, M. A. Hammond, and J. M. Wallace, "Structural and mechanical improvements to bone are strain dependent with axial compression of the tibia in female c57bl/6 mice," *PloS one*, vol. 10, no. 6, p. e0130504, 2015.
- [19] M. A. Hammond, A. G. Berman, R. Pacheco-Costa, H. M. Davis, L. I. Plotkin, and J. M. Wallace, "Removing or truncating connexin 43 in murine osteocytes alters cortical geometry, nanoscale morphology, and tissue mechanics in the tibia," *Bone*, vol. 88, pp. 85–91, 2016.
- [20] R. Ritchie, K. Koester, S. Ionova, W. Yao, N. Lane, and J. Ager, "Measurement of the toughness of bone: a tutorial with special reference to small animal studies," *Bone*, vol. 43, no. 5, pp. 798–812, 2008.

5. CONCLUSION AND FUTURE DIRECTIONS

The purpose of the studies in the preceding chapters was to observe the effects of tibial loading on bone quality. Initially, this was explored through injection with BAPN as a means of inducing osteolathyrism, a collagen quality-based bone disease that acts by preventing the formation and maturation of enzymatic cross-linking in bone. However, a functional disease was not observed at the relatively low dose chosen despite the long course of treatment. After increasing the dose of BAPN, an overt disease state was still not observed (only mild effects). However, there were many significant interaction effects, suggesting that while no overt functional disease was achieved, the injections with BAPN altered the bone's response to loading. Loaded BAPN tibiae increased mass by endocortical contraction, whereas the CON mice increased bone mass by periosteal expansion.

Although there were some mild effects of BAPN, the lack of a functional disease at both the low and high dose levels suggests that inducing a BAPN disease state should be pursued by alternate means. One such method is through the food the animals eat, which has the added benefit of maintaining a more constant concentration of the drug in the body as compared to the bolus injection given in these studies. Future studies will explore inducing a disease state by this alternate method.

While the lack of a functional disease made it difficult to assess the role of loading on bone quality in a disease state, the effects of loading observed in the CON mice in Chapters 2 and 3 led to the study in Chapter 4. Namely, in the first BAPN study, loading caused improvements in mass and structural-level mechanical properties. However, after normalizing to cross-sectional area, the effects of load were milder. In addition, there was no effect of load on fracture toughness parameters. Together, these results suggested that the bone increased mechanical strength primarily through increases in mass, and not quality. In addition, the mice in the

second BAPN study (Chapter 3) also showed signs of limping despite changing the load level during the rest period. As a result, Chapter 4 assessed different loading regimes as a means of decreasing pain and improving bone quality in the animals.

In Chapter 4, four different loading regimes were explored. A greater pain response (as assessed by limping, swollen ankles, and stiff joints) was observed in the group that was loaded for three days in a row and held at the high load level during the rest period. For that group, although there was a robust response in terms of bone mass, there was a lack of improvement in bone quality, as assessed by fracture toughness. Overt damage of the proximal tibia was also observed in that group. In contrast, the group that was only loaded twice per week showed little to no pain throughout the study. There were some (mild) effects of loading on bone mass, but none on bone quality. The best loading regime for quantity and quality-based improvements was found to be loading every other day (3 times per week). Mice in this group showed mild signs of limping, robust response of loading on bone mass, and a trend toward increasing bone quality. Future studies will address if decreasing the number of cycles in a loading bout can prevent all limping (even mild) while still maintaining a robust response.